

ALMA MATER STUDIORUM - UNIVERSITÀ DI BOLOGNA

SCUOLA DI INGEGNERIA E ARCHITETTURA

Dipartimento di Ingegneria dell'Energia Elettrica e dell'Informazione

CORSO DI LAUREA MAGISTRALE IN INGEGNERIA GESTIONALE

MASTER'S THESIS

In

ALGORITHMS FOR DECISION MAKING M

**A Liner Shipping Speed Optimization Model
to Reduce Bunker Cost and Pollutants Emitted**

Candidate: Pier Cesare Rossi

Supervisor: Enrico Malaguti¹

Co-supervisors: Stefan Røpke², Line Blander Reinhardt³, Valentina Cacchiani¹

¹ Alma Mater Studiorum Università di Bologna

² Technical University of Denmark

³ Aalborg University Copenhagen

Abstract

Environmental impact has become one of the most relevant issues in liner shipping during the recent years. Maritime shipping is responsible for the 2.7 per cent of the world CO₂ emissions, of which 25 per cent is attributable to container ships. This business also produces a significant quantity of sulphur, a very dangerous substance for human health, especially if it is emitted in areas next to the coast. At the same time, bunker cost represents the biggest portion of the operational cost of a shipping company. Slow steaming is a cheap and effective strategy from both save pollutants emissions and bunker cost. Moreover, it can be immediately put into practice. This report introduces a Mixed Integer Programming Model to solve the Liner Shipping Routing and Speed Optimization Problem (LSRSOP). The final goal is to find the best route and to optimize the the sailing speed of the vessel considering the Emission Control Areas and maximum transit times between ports. Two Heuristic Methods -the 2-Steps Method and the Simulated Annealing- are proposed to solve big instances that would require too much running time to be solved until optimality. Both of them use a Hill-Climbing Algorithm that generates a slight different route from a given one. A Bi-Objective Function Model has been designed for instances whose the optimal solution can be found in reasonable time. It considers the operative cost of the vessel and the external cost of emissions. The results show efficient solutions that are the "golden line" between the most convenient solution for the company and the most sustainable solution.

Contents

List of Figures	v
List of Tables	vii
List of Algorithms	ix
1 Introduction	1
1.1 Project Scope	4
1.2 Contributions	5
2 The Liner Shipping Business	7
2.1 Shipping Company Cost Structure	7
2.2 The Effect of Sailing Speed on Bunker Consumption	8
2.3 Pollutants Emissions by Liner Shipping	10
2.4 The Liner Shipping Routing and Speed Optimization Problem	12
3 Literature Review	15
4 Modeling	17
4.1 The Traveing Salesman Problem	17
4.2 Linearization Method of the Bunker Consumption Function	18
4.3 The Liner Shipping Routing and Speed Optimization Model	20
4.4 Mathematical Model for the LRSOP	25
5 Data Description	29
6 Solution Methods and Results	35
6.1 Heuristic Approach	36
6.2 Two-Steps Method	36
6.2.1 Routes Generation Algorithm	37
6.2.2 Speed Optimization Problem	37
6.2.3 Hill-Climbing Algorithm	40
6.2.4 Two-Steps Method Results	42
6.3 Simulated Annealing	44
6.3.1 Simulated Annealing Tuning	44
6.4 Optimal Solution	47
6.4.1 User Cut: Subtours	47
6.4.2 Subtour User Cut Result	50
6.4.3 User Cuts: Lower Bounds for Delays and Transit Times	52
6.5 Bi-Objective Function Model	55
6.5.1 Bi-Objective Model Result	57

CONTENTS

6.5.2 The shipping company point of view 59

6.5.3 The environmental point of view 60

6.6 Sensitive Analysis for Delay Cost per Hour per FFE 63

6.7 As-is/To-be Analysis 64

7 Conclusion 67

List of Figures

1.1	The relationship between the world GDP growth and seaborne trade growth (Source: Clarkson Research Services Ltd).	1
1.2	International seaborne trade, selected years (millions of tons loaded) (UN, 2015).	2
1.3	Structure of the international seaborne trade in percentage (UN, 2015).	2
1.4	Global Ecological Footprint by component vs Earth's biocapacity (green line), 1961-2012	3
1.5	Map of Emission Control Areas in Europe and North America (Fagerholt, Gausel, et al., 2015a)	3
1.6	New IMO's regulations from 2020.	4
1.7	The WestMed Service, transporting containers between U.S. east coast and the western Mediterranean.	5
2.1	BW380 and BW0.1S price (BunkerWorld, 2017)	8
2.2	Sensitivities for the calendar year 2017 for four key value drivers (MaerskLine, 2017)	8
2.3	Relation between sailing speed and bunker consumption.	9
2.4	Total, Bunker and Fleet Cost in Relation to Speed.	9
2.5	Emissions of CO2 from shipping compared with global total emissions for 2007 (IMO, 2009)	10
2.6	Planning Levels for Liner Shipping (Fagerholt, 2001).	12
2.7	The relationship between roundtrip distance, required vessel speed and the number of employed vessels. (Notteboom and Vernimmen, 2009a)	13
2.8	Sailing time-bunker consumption relation	14
4.1	Gap between the Relaxed Solution and the Optimal Integer Solution	18
4.2	Fuel consumption in function of the sailing time (left); fuel consumption approximated by 15 secants (right)	19
5.1	BW380 and BW0.1S cost (BunkerWorld, 2017)	33
6.1	Length comparison between route a and route b	41
6.2	Example of Hill-Climbing Algorithm: given a maximum number of 4 ports exchanged, 3 of them are actually switched	41
6.3	Example of 2-Step test for [15Wor] instance, maximum ports exchanged = 3; on the x-axis is the running time from 0 to 300 seconds.	44
6.4	Example of SA test for [15Wor] instance, $r = 0.1$; on the x-axis is the running time from 0 to 300 seconds.	46
6.5	Example of SA test for [20Atl] instance, $r = 0.001$; on the x-axis is the running time from 0 to 300 seconds.	46
6.6	Use of lazy constraints and user cuts in an integer linear program	47
6.7	Known relationships between twenty-four ATSP formulations (Öncan et al., 2009)	48
6.8	First (picture on the left) and second (picture on the right) subtours found from Algorithm 3 for [10Ame] instance run	49
6.9	Edgeworth-Pareto hull (Ehrgott et al., 2016)	56
6.10	The ϵ -constraint method scalarization (Ehrgott et al., 2016)	57

LIST OF FIGURES

6.11 Bi-Objective function model Result: Pareto frontier of 10 American Ports 59

6.12 Average sailing speeds in Knots for the solutions on the Pareto Frontier 60

6.13 CO2 savings in kg of the efficient solutions compared with the company most convenient solution 62

6.14 SO2 savings in ton of the efficient solutions compared with the company most convenient solution 63

List of Tables

2.1	CO2 Emissions of Different Transport Means (Source: Swedish Network for Transport and the Environment).	10
2.2	Bottom-up CO2 emissions from international shipping by ship type 2012 (IMO, 2014)	11
4.1	LSRSOP Sets	22
4.2	LSRSOP Parameters	22
4.3	LSRSOP Parameters 2	23
4.4	LSRSOP Emission Parameters	24
4.5	LSRSOP Variables	25
5.1	World ports instance description	30
5.2	Atlantic ports instance description	31
5.3	American ports instance description	32
5.4	Panamax 2400	32
5.5	Percentage of the leg inside SECA	33
5.6	Example of values to calculate the bunker consumption (see Section 4.2 for further explanations)	34
5.7	Example of MTT values	34
5.8	Example of quantity transported in FFE	34
6.1	SOP Sets	38
6.2	SOP Variables	39
6.3	2-Steps Method result, instance: 15 World ports	43
6.4	2-Steps Method result, instance: 20 Atlantic ports	43
6.5	Best values of the tests of Simulated Annealing Analysis for 20 Atlantic ports instances; tuning the final temperature coefficient	45
6.6	Best values of the tests of Simulated Annealing Analysis for 15 World ports instances; tuning the final temperature coefficient	46
6.7	Subtours User Cuts results compared with the complete model (4.18-4.35)	51
6.8	Optimal solution for both the objective functions, instance: 10 American ports	51
6.9	Optimal solution for both the objective functions, instance: 10 Atlantic ports	52
6.10	Maximum Delay User Cuts results compared with the complete model (4.18-4.35)	54
6.11	Transit Time User Cuts results compared with the complete model (4.18-4.35)	54
6.12	Maximum Flow User Cuts results compared with the complete model (4.18-4.35)	55
6.13	Bi-Objective Model Result, example of dominate points, instance: 10 American Ports . .	58
6.14	Bi-Objective function model result, instance: 20 Atlantic Ports	58
6.15	Bunker and delay penalty costs for the solutions on the Pareto Frontier	60
6.16	CO2 and SO2 emissions of the Pareto Frontier solutions	61
6.17	Sensitive analysis for the cost of delays, instance: 10 American ports	64
6.18	Sensitive analysis for the cost of delays, instance: 10 Atlantic ports	64
6.19	Parameters comparison between As-Is and To-Be scenarios	65
6.20	As-Is and To-Be analysis for 10 Atlantic ports instance, obj: operative cost	65

LIST OF TABLES

6.21 As-Is and To-Be analysis for 10 American ports instance, obj: operative cost . . .	66
---	----

List of Algorithms

6.1	Routes Generation Algorithm	37
6.2	Hill-Climbing Algorithm	42
6.3	Subtours in LP Relaxation Algorithm	50
6.4	Lower Bounds for Delays and Transit Times Algorithm	53
6.5	Non-dominated points on the Pareto Frontier research	57

Chapter 1

Introduction

Maritime shipping industry enables the trade of a huge amount of goods all over the world. UN (2015) estimates indicate that global seaborne shipments have increased by 3.4 per cent in 2014, at the same rate as in 2013. The total volume moved was 9.84 billion tons. Maritime shipping made its fortune thanks to the globalization of the last decades. The worldwide economy keeps growing and it has given the rise to the need of a more dynamic and efficient market. This is due to the participation of developing countries in the maritime shipping trade as well (UN, 2015). A general view of the relationship between world Gross Domestic Product (GDP) and the volume of seaborne trade is provided by DNV (Figure 1.1). The two trends are closely linked: in periods of low GDP growth, as during the last crisis of 2009, the volume of seaborne trade shrinks.

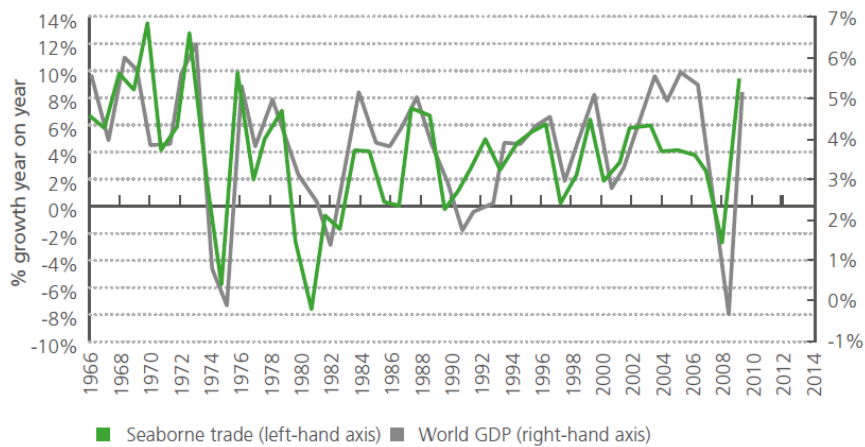


Figure 1.1: The relationship between the world GDP growth and seaborne trade growth (Source: Clarkson Research Services Ltd).

Ocean shipping's economies of scale enable cheap goods transportation for long distances which would not be feasible with costlier, less efficient means of transport. It allows 80 per cent of global trade (Premti, 2016) by volume and, for this reason, it remains decisive for the global economy development. At the same time, managing this business is still quite hard because a lot of factors have to be taken into account. Indeed disruptions, bad weather conditions and port congestions can cause delays and particular national laws can sometimes hinder this business. Looking at the data showed above, it is clear that maritime transport can have a determinant role in the world's trade integration. This report wants to enhance the growth of this sector, that means optimizing the cost structure related to it abiding by pollutants emissions restrictions issued by the International Maritime Organization. A comparison will be done between the company and the

environmental perspective: adjusting the sailing speed have totally different outcomes if one wants to minimize the operative costs or the pollutants emitted.

Bulk shipments moved 4.55 billion tons in the last years and they are often transported as tramp shipping; hence it is not treat in this study. “Other dry cargo” accounted for 35.2 per cent of all dry cargo shipments. Containerized trade, which accounts for about two thirds of “other dry cargo”, is expected to increase by 5.6 per cent, taking reaching a total of 1.63 billion tons (Figure 1.2). This report analyses container shipping since it represents one of the biggest portion of the seaborne trade (Figure 1.3) and, as Section 2.3 shows, it is responsible of a consistent quantity of pollutants emitted. Moreover, unlike crude oil ships, routes of container vessels are subjected to maximum transit times constraints between ports, therefore sailing speed optimization of these vessels is an interesting subject of study.

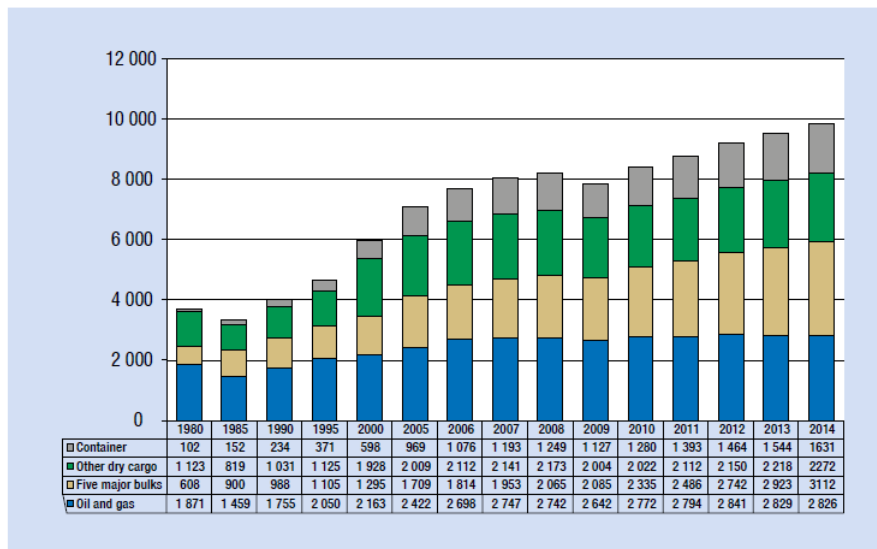


Figure 1.2: International seaborne trade, selected years (millions of tons loaded) (UN, 2015).

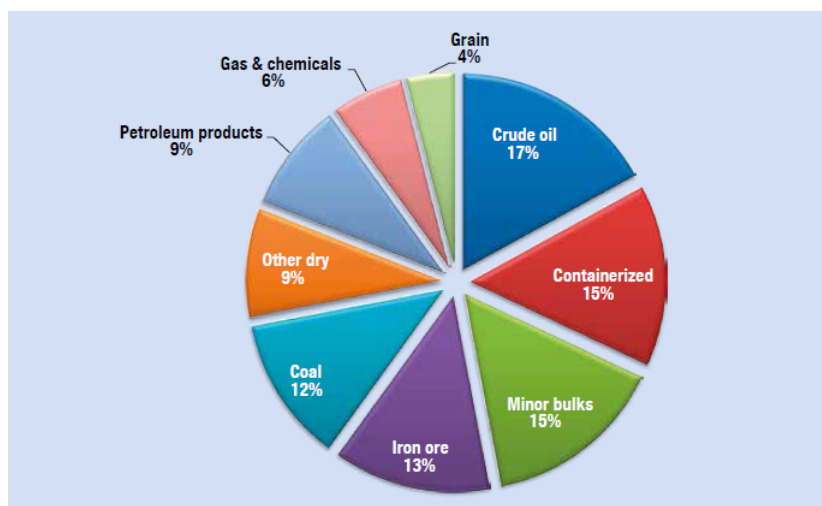


Figure 1.3: Structure of the international seaborne trade in percentage (UN, 2015).

In recent years, many regulations have been issued to limit the pollutants emissions from maritime transportation. Combustion of fuel produces carbon dioxide (CO₂), oxides of sulphur

(SO_x), volatile organic compounds (VOCs), ozone, particulate matter (PM) and oxides of nitrogen (NO_x) (Cullinane et al., 2013). This report will focus on CO₂ and SO₂ because they are the most detrimental emissions. CO₂ is a well known greenhouse gas, hereafter GHG, responsible for the climate change. Even if SO₂ is not a GHG, it is detrimental for humans lungs and acute exposure can cause respiratory problems, even bronchitis and tracheitis (McGranahan et al., 2012). It has been shown that SO₂ in the air increases death rates. Mortality increased by approximately 40% in 2012 due to trade-driven growth in shipping emissions (Corbett et al., 2007).

At the same time, shipping emissions, together with other humans activities, contribute to the tremendous and damaging impact on the planet. Carbon emission is the main component of the humanity's Ecological Footprint, i.e. human demand on the ability of the planet to provide renewable resources and ecological services (Figure 1.4). We are currently using 60 per cent more resources than the planet is able to regenerate (WWF, 2017).

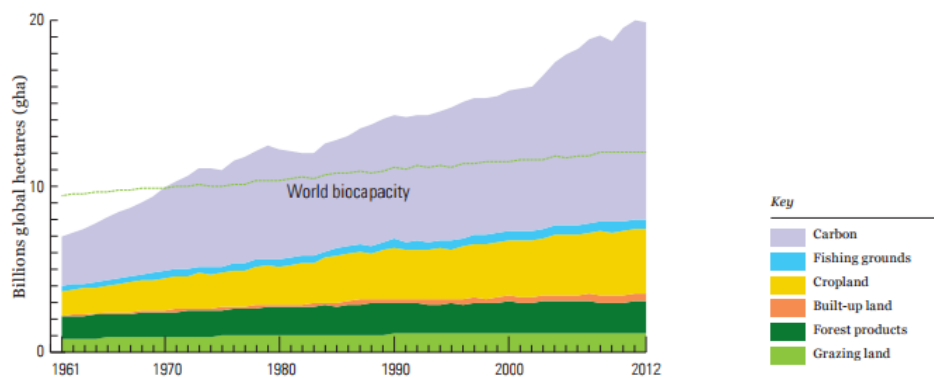


Figure 1.4: Global Ecological Footprint by component vs Earth's biocapacity (green line), 1961-2012

Therefore, for both health and environmental reasons, the International Convention for the Prevention of Pollution defined the North American, US Caribbean, North Sea and Baltic Sea as Emission Control Areas (ECAs) to limit SO_x and NO_x in zones where people live. A threshold of 0.1 per cent of sulphur content in the fuel has been set in those areas. In other zones the sulphur content limit is 3.5 per cent. Shipping companies will have to use a more refined and expensive fuel in ECAs to respect the regulation. ECAs are shown in Figure 1.5. Adjusting sailing speed is an effective strategy to optimize bunker consumption both inside and outside ECAs, that means optimizing bunker cost. Moreover, it does not require additional investments.



Figure 1.5: Map of Emission Control Areas in Europe and North America (Fagerholt, Gausel, et al., 2015a)

At the same way, the new regulations entering into force in January 2020 are interesting (Figure 1.6). In addition to the 0.1 per cent sulphur limit in the Sulphur ECAs, the global limit will be 0.5 per cent instead of the current 3.5%. The European Union Sulphur Directive imposes a maximum 0.5% sulphur content for ships in all EU seas by 2020, and a 0.1% limit in ports. China is taking a staged approach and, in conjunction with Hong Kong, it may tighten the limit to 0.1% (DNV, 2012).

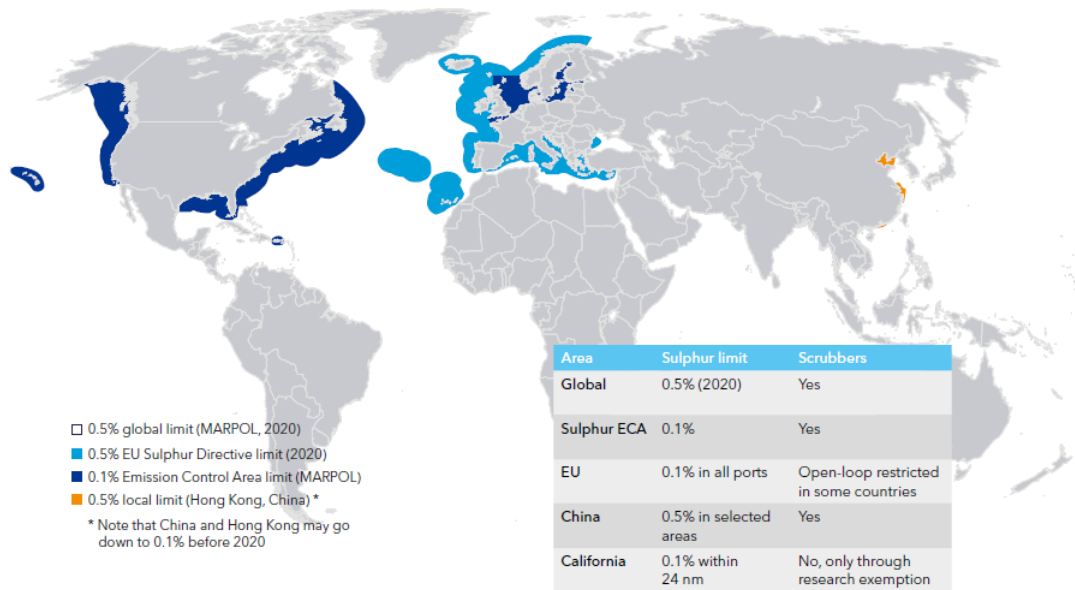


Figure 1.6: New IMO's regulations from 2020.

1.1 Project Scope

Liner shipping is the business of carrying goods all over the world taking into account time restrictions due to national and international policies and goods that lose value over time. A container shipping network is based on a fixed schedule (usually one week) with a predetermined trip duration. The trip duration is a multiple of a week and the number of weeks needed is equal to the number of vessels employed so that every port is visited once a week. In other words, a different vessel starts its round trip at the beginning of each week. An example of network is provided by Pisinger 2014 and it is shown in Figure 1.7. The WestMed Service lasts 6 weeks and therefore 6 vessels are required.

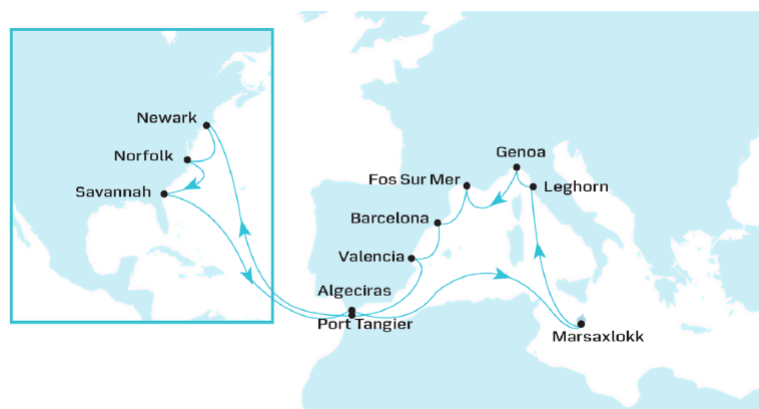


Figure 1.7: The WestMed Service, transporting containers between U.S. east coast and the western Mediterranean.

The purpose of this study is defining a model to solve the Liner Shipping Routing and Speed Optimization Problem (LSRSOP). The optimal solution finds the best route and the sailing speed on each leg that minimize the operative cost of the vessel. The model has to consider maximum transit times between ports and the above described ECAs. Moreover, it is also possible to find the optimal solution minimizing the pollutants emitted. In this case, the external cost of emission will be calculated. By minimizing the two objective functions, two different solutions are found: if the operative cost of the vessel are minimized, the average sailing speed will be high in order to meet as delivery schedules as possible; if the external cost of emission is minimized, the vessel will sail slowly in order to reduce the fuel consumption, that is limit emissions. The final purpose of this report is to analyse both the environmental and the shipping company points of view.

Chapter 2 describes the cost structure of the shipping company with particular emphasis on the impact of the bunker cost. In the same Chapter, the relation between sailing speed and bunker consumption is shown; Section 2.3 shows relevant data about CO₂ emissions and describes in depth the Emission Control Areas. Finally, Section 2.4 describes the Liner Shipping Routing and Speed Optimization Problem that will be modelled in this study.

Chapter 3 contains the literature review where the main articles about liner shipping problems are described, as well as some relevant papers that have been useful to propose the solution methods of this study.

Chapters 4 and 5 describe the mathematical formulation of the model and the instances used to run the solution methods respectively.

Chapter 6 shows the solution methods proposed to solve the LSRSOP. For big instances it is not possible to find optimal solutions, therefore two Heuristic Methods have been proposed (Sections 6.1-6.3.1). Section 6.4 is dedicated to the description of some User Cuts that had the purpose of tightening the lower bound and decreasing the running time. Finally, Section 6.5 compares the company prospective and the environmental point of view with a Bi-Objective Function Model and Section 6.7 shows the result of the As-Is/To-Be Analysis considering the new regulations from 2020.

1.2 Contributions

This project is a master's thesis developed in the *Engineering Management Department* of the *Technical University of Denmark*. It will be delivered to the *University of Bologna* to obtain a Master degree in *Management Engineering*. The project will be defended in both universities.

However, the report also represents a value for the academic society by:

- Presenting a model for the LSRSOP that includes transit time and Emissions Control Areas restrictions;
- Providing heuristic methods to solve large instances;
- Suggesting different approaches to decrease the running time to find the optimal solution;
- Defining a Bi-Objective Function Model to find optimal solutions that consider both the company and the environmental point of view;
- Evaluating the variation of penalty cost of the company for different values of the cost per hour of delay;
- Evaluating the SO₂ savings due to the new IMO's regulation from 2020.

Chapter 2

The Liner Shipping Business

The business of liner shipping is an important element of the world trade market. It consists of the transportation of different goods all over the world by using container vessels. A service is a round trip network that connects a given set of ports. Carriers would choose the most profitable port calls but, at the same time, they have to accommodate the transit time limits between ports and environmental and national regulations; that is why the research about liner shipping business is challenging and interesting.

In Section 2.1 the cost structure of this business is described, with a particular focus on the bunker cost, that is the biggest cost of a vessel. The relation between sailing speed and bunker cost is described in Section 2.2. Section 2.3 shows the environmental impact related to liner shipping and the regulations that will be considered in the mathematical model. The description of the Liner Shipping Routing and Speed Optimization Problem is reported in Section 2.4.

2.1 Shipping Company Cost Structure

Shipping companies are interested in understanding their cost structure in order to study efficient strategies to optimize it. On the other hand, policy makers collect information about maritime trade costs to issue useful regulations. A global container shipping network has a very high total cost (order of billion according to MaerskLine (2017)). Therefore, even a small improvement of the network's management can have a significant impact.

The cost of a carrier can be divided into fleet cost, cargo-handling cost and administrative cost (30% according to Stopford (2009)). The biggest cost is the bunker cost (part of the fleet cost). It accounts for 35%-50% of the overall cost and it overtakes both capital cost (acquiring and financing a vessel) and operational cost (crew, maintenance and insurance) (Brouer et al., 2013). Moreover, if the fuel price is around 500 [USD/ton], bunker cost can be three quarters of the total operating cost (Ronen, 1982a). Bunker cost assumes different values according to the fluctuation of the oil price: Figure 2.1 shows the fluctuations of two types of fuels. "BunkerWorld 380 Index" (BW380) and "Maximum 0.1% Sulphur - Distillate Index" (BW0.1%S) are the fuels chosen for this study. They have different sulphur contents and they have to be used in different sea areas in order to comply with the environmental regulations.

An example of how much bunker cost is decisive on the balance sheet of a company, is given by MaerskLine (2017): a variation of ± 100 [USD/ton] has an effect of ± 400 million[USD] (Figure 2.2).

For these reasons, shipping lines work to keep bunker cost under control and to reduce it. They can undertake some strategies such as: using cheaper grades of bunker fuel (like Intermediate Fuel Oil 500 instead of Intermediate Fuel Oil 380) (Notteboom and Vernimmen, 2009a), re-designing new vessels and controlling the speed. This report will be focused on the third alternative called *slow steaming*. The main advantage of the slow steaming strategy is that, unlike the other stated options, it does not require any additional investment to shipping companies.

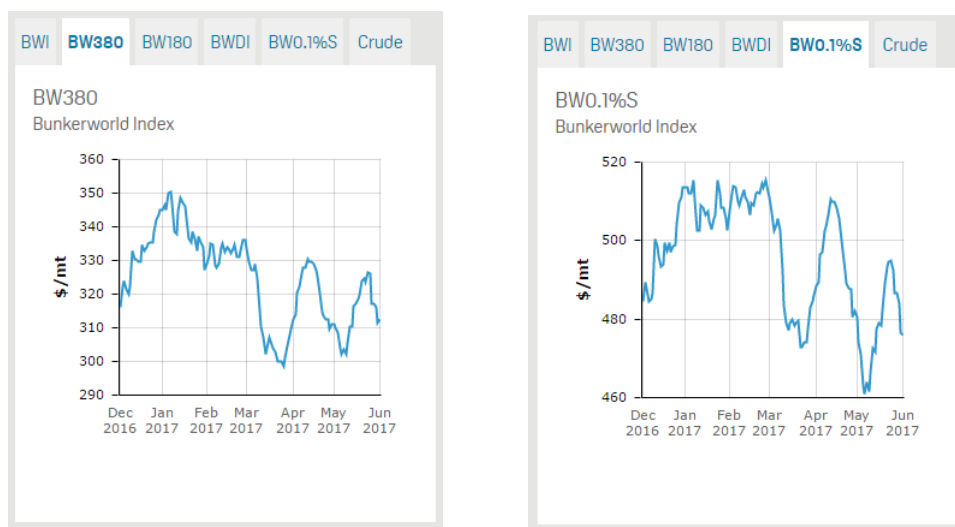


Figure 2.1: BW380 and BW0.1S price (BunkerWorld, 2017)

Factors	Change	Effect on A.P. Moller - Maersk's underlying result
Oil price for Maersk Oil ¹	+/-10 USD/barrel	+/-USD 0.26bn
Bunker price	+/-100 USD/tonne	-/+USD 0.4bn
Container freight rate	+/-100 USD/FFE	+/-USD 1.1bn
Container freight volume	+/-100,000 FFE	+/-USD 0.1bn

Figure 2.2: Sensitivities for the calendar year 2017 for four key value drivers (MaerskLine, 2017)

2.2 The Effect of Sailing Speed on Bunker Consumption

Bunker consumption can vary according to the sailing speed, the fuel cost, the draft of the vessel, the weather condition and the design of the vessel. Figure 2.3 shows the relationship between speed and fuel consumption of four different type of container vessels: 3000 twenty-foot equivalent units (3000-TEU ships for short), 5000-TEU ships and 10000-TEU ships (Notteboom and Vernimmen, 2009a). A change in speed causes a dramatic increase of fuel consumption. For example, increasing service speed from 16 to 20 knots, using a 5000 TEU container, has a variation of 15000 [USD/day]. Therefore the sailing speed is a key determinant of bunker cost and consumption.

Sailing at a high speed allows shipping companies to move a bigger amount of cargos over a given period. On the other hand, fuel is the largest cost in container ship operations. Ocean carriers have a huge interest in reducing the amount of fuel their ships consume, and have undertaken several initiatives to improve fuel efficiency from reducing vessel speed, to sharing their vessels with other carriers, to building larger ships that are more energy efficient per unit of cargo carried. Therefore, in liner shipping the trade-off coming from this situation is between reducing bunker consumption through speed reduction and achieving competitive delivery times to maximize revenues (Brouer et al., 2013). Indeed, the cargo ship can slow steam to save fuel or accelerate to accommodate the transit time restrictions and increase the service level.

As said in the previous section, it is possible to reduce bunker cost by installing new technological components on the vessels. However, this entails high investments. A less expensive strategy is the logistic-based "slow-steaming" that simply means reducing sailing speed. It has a high relevance for the pollutants emissions reduction too (in-depth analysis in Section 2.3). Slow steaming was

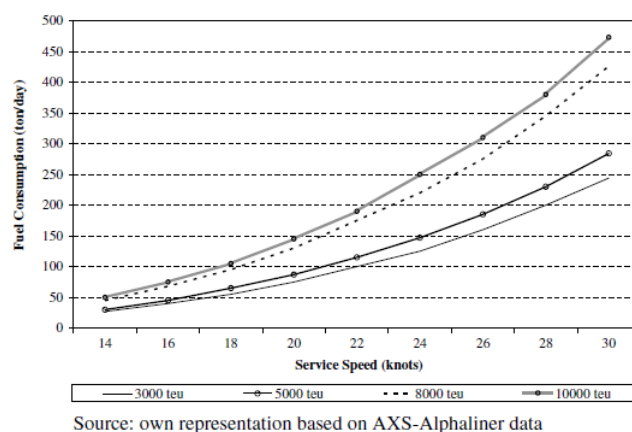


Figure 2.3: Relation between sailing speed and bunker consumption.

introduced in 2007 by Maersk Line to cut CO₂ emissions per container by 12.5% from 2007 to 2009. The shipping company claims that a speed reduction of 20 per cent saves 40 per cent less of fuel. To guarantee the same route frequency and compensate the lower speed 1 or 2 extra vessels are required (MaeskLine, 2010).

Liner companies are sometimes unwilling to apply the slow steaming strategy to reduce operating cost because this causes an increase of inventory cost. Inventory cost is strictly tied to the transit time of the vessel and it has a high impact especially for high-value goods transportation (Figure 2.4). This is even more an issue for perishable goods transportation. Nevertheless, reducing speed to obtain sailing cost saving is preferable than giving priority to inventory cost reduction since the latter is a discrete function.

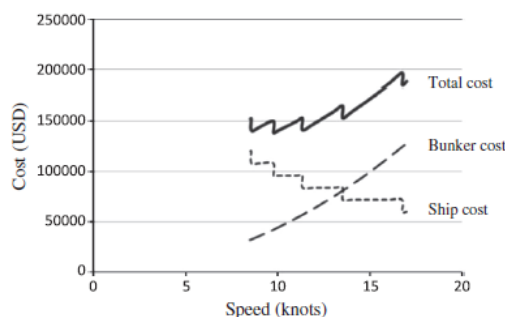


Figure 2.4: Total, Bunker and Fleet Cost in Relation to Speed.

Another drawback of slow steaming is that having high transit times may make other means of transport more convenient. This can happen especially in short sea trades like Europe.

It is clear that bunker consumption is a non-linear function of speed and approximations are used to estimate it in mathematical models. As Psaraftis et al. (2013) show, bunker consumption can be equal to $A + Bv^n_{(i,j)}$, where A , B and n are input parameters such as $A \geq 0$, $B > 0$, $n \geq 3$ and v is the speed on (i, j) leg connecting two ports. Otherwise, bunker consumption can be proportional to $(w_{(i,j)} + L)^{2/3}$ for a given speed, where L is the weight of the vessel and $w_{(i,j)}$ fuel on board (Barrass, 2004).

Another formula, the one will be used in this study, is a cubic function described by Brouer et al. (2013):

$$F(s) = \left(\frac{s}{v_*^F} \right)^3 \cdot f_*^F \tag{2.1}$$

where s is a generic speed between the minimum speed s_{min}^F and the maximum speed s_{min}^F of vessel F , v_*^F is the design speed and f_*^F is the fuel consumption at design speed. The study of Wang et al. (2012b) proves that this cubic function is a good approximation of bunker consumption.

2.3 Pollutants Emissions by Liner Shipping

Reducing the operating cost of the vessel is not the only advantage coming from adjusting sailing speed. The environmental impact of liner shipping has a high relevance as well. According to the study of IMO (2009), maritime shipping is responsible for the 2.7 per cent of the world CO2 emissions (Figure 2.5), of which 25 per cent is attributable to container ships (IMO, 2014).

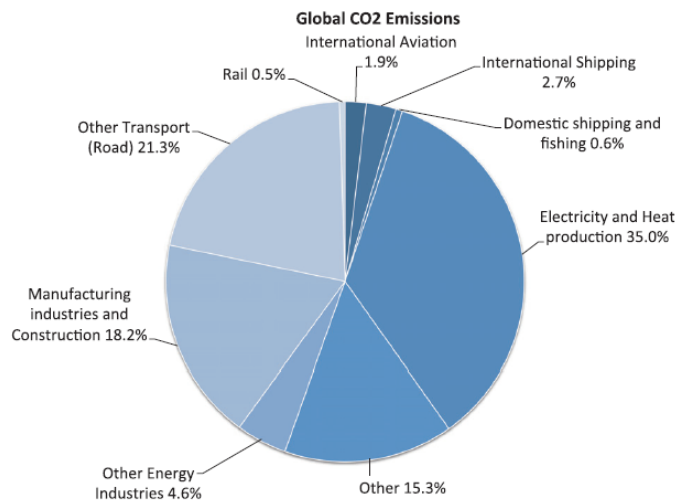


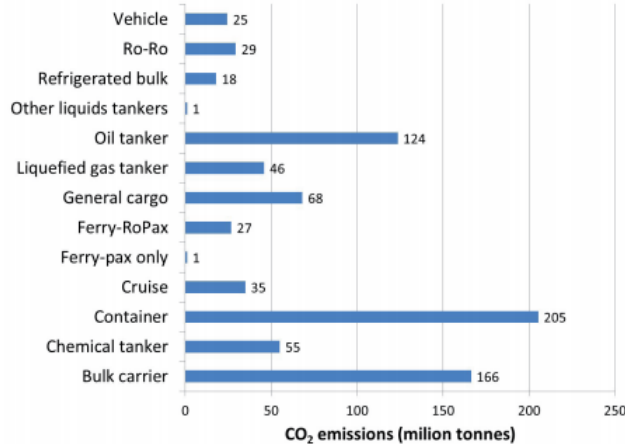
Figure 2.5: Emissions of CO2 from shipping compared with global total emissions for 2007 (IMO, 2009)

Table 2.1 clearly shows that liner shipping is the most carbon-efficient form of transporting goods. In this case, it is compared with diesel train, truck and air cargo. However, the fuel used today by the vessels and for the other means of transport is still polluting in terms of SOx and NOx; the pollution can be reduced even more thanks to environmental regulations and tactical decisions such as slow steaming. This means that liner shipping business has a great potentiality to sustain the global eco-friendly trade development.

Mode	CO ₂ (gr/tonne-km)	SO ₂ (gr/tonne-km)	NO _x (gr/tonne-km)
Boeing 747-400	552	5.69	0.17
Heavy truck	50	0.31	0.00005
Rail-diesel	17	0.35	0.00005
Rail-electric	18	0.44	0.10
S-type container vessel (11,000 TEU)	8.35	0.21	0.162

Table 2.1: CO2 Emissions of Different Transport Means (Source: Swedish Network for Transport and the Environment).

This report will be focused on liner shipping since this is the most CO2 emissions grade category in the maritime sector (Table 2.2). Psaraftis et al. (2013) state that reducing sailing speed will drastically reduce emissions too.

Table 2.2: Bottom-up CO₂ emissions from international shipping by ship type 2012 (IMO, 2014)

Carbon dioxide is one of the GHG responsible for the Earth temperature increment. The Kyoto Protocol, adopted in 1997, is an international treaty that commits the 175 State Parties to reduce greenhouse emissions in industrialised countries. However, aviation and shipping emissions are difficult to calculate and they are omitted from the Protocol. Instead, Article 2.2 of the Kyoto Protocol imposes that these two industries have to respect the regulations imposed by the International Civil Aviation Organization and the International Maritime Organization, hereafter IMO. As stated on IMO web site, “IMO has promoted the adoption of some 50 conventions and protocols and adopted more than 1,000 codes and recommendations concerning maritime safety and security, the prevention of pollution and related matters” (IMO, 2013).

One of the most important convention was the International Convention for the Prevention of Pollution from ships, hereafter MARPOL. In this meeting a new regulation for sulphur content in the fuel oil was issued: no more than 0.10 per cent allowed instead of 1 per cent. This limit is valid from January the 1st 2015 inside the ECAs: North American, US Caribbean, North and Baltic Seas. The zones belonging to ECAs are illustrated in Figure 1.5. Carriers must use a more expensive fuel to sail in ECAs to respect the sulphur emission limit. The consequence of the regulation is that ships that sail outside the ECAs use a cheap fuel called heavy fuel oil (HFO), and inside they use the marine gas oil (MGO), more expensive but with low sulphur content (Fagerholt, Gausel, et al., 2015a).

An alternative to HFO is the distillate Liquefied Natural Gas (LNG). It is a promising solution since it allows cost saving in addition to comply with IMO’s regulations. Indeed, even if the CO₂ coefficients of HFO and LNG are quite similar (3.1144 and 3.206 [kgCO₂/ton] respectively) (Kontovas, 2014), it has a lower SO₂ percentage content. To calculate the SO₂ emissions, it is necessary to multiply the total bunker consumption [ton/day] by the percentage of sulphur present in fuel and by a factor of 0.02. The factor of 0.02 is derived from the chemical reaction of sulphur with oxygen. Acciario (2014) calculated the optimal deferral time for investment on switching to LNG. The study suggests to invest in the near future but it states that a decrease in time spent inside the SECAs would discourage the investment. However, new regulations will take into force in 2020 (Figure 1.6): this definitely makes LNG an optimal response to emission’s limits standards.

To limit GHG emissions, IMO issued Market Based Measures by investing in more fuel efficient ships and technologies. These measures entered into force on January the 1st 2013. Liner companies have to clean the underwater parts of the ships and the propeller more often and to adopt eco-friendly technologies such as waste heat recovery systems (IMO, 2011). Moreover, the attained Energy Efficiency Design Index, measured in [gCO₂/(ton · mile)] has to be lower than a threshold. The formula is provided by Psaraftis et al. (2013):

$$AttainedEEDI \leq RequiredEEDI = (1 - X/100) \cdot a \cdot DWT^c \quad (2.2)$$

where X is a reduction factor that varies on when the ship was built, DWT is the dead-weight of the ship, a and c are parameters defined by IMO by a regression analysis.

A drawback of this limit is that the left-side of equation 2.2 is function of the design speed and the right side is independent. This means that ship constructor could install a lower power to decrease the design speed with the result of underpowered vessels will burn more fuel (and emit more CO₂) to maintain the same speed of normal vessels while satisfying the EEDI threshold requirement.

Since bunker consumption is directly proportional to pollutants emissions, controlling these emissions by adjusting sailing speed is a reasonable option. Slow steaming is part of *green logistic*, a wider concept introduced by Sbihi et al. (2010). The authors state that optimizing capacity utilization and sailing speed of vessels will ensure a positive effect on the environment by reducing pollutants emitted. Now the question is: how can policy makers encourage shipping companies to diminish pollutants emitted? Instituting speed limits is not a useful strategy because it can have several drawbacks. Firstly, as explained in Section 2.2 the inventory cost will increase or land-based transports can become a valid substitution; secondly, building more vessels in response to delivery delays can increase CO₂ in shipping and recycling (Psaraftis et al., 2013). Therefore, it is necessary to find the right balance between operating cost and environmental impact while setting speed. Sailing speed is a key determinant for both shipping costs and environmental sustainability.

2.4 The Liner Shipping Routing and Speed Optimization Problem

Patrick M Alderton (2004), Stopford and Brouer et al. (2013) provide an in-depth and historical analysis of liner shipping. The mathematical model proposed in this study to solve the Liner Shipping Routing and Speed Optimization Problem (LSRSOP) is based on some features described by the cited authors. Figure 2.6 shows the three decision-making levels for liner container shipping companies: strategic, tactical, and operational (Pesenti, 1995). At the strategic level, a liner container shipping company makes long-term decisions, tactical decisions are made every three to six months and operational decision are the ones taken during the route due to problems that may arise. The sailing speeds between each pair of ports are decided simultaneously with the routing and scheduling decisions.

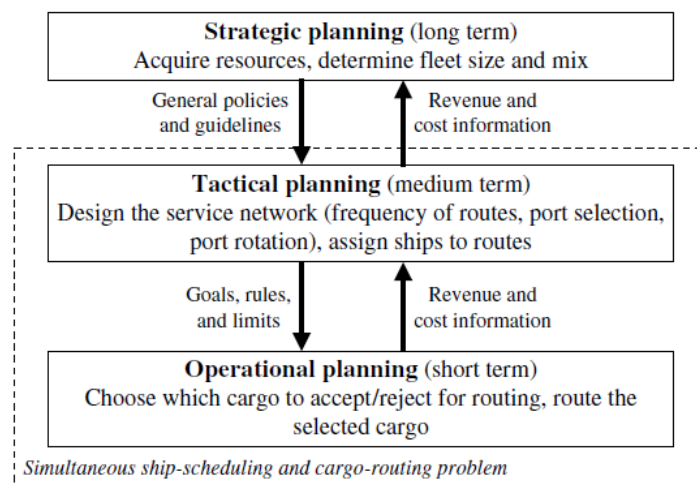


Figure 2.6: Planning Levels for Liner Shipping (Fagerholt, 2001).

The features of the mathematical model to solve the LSRSOP are described in this Section. Liner shipping consists of the transportation of goods with container vessels. A *service* or route, is a sequence of port calls. The round trip service is the simplest service in which every port is visited

once. The round trip can have different sizes. A trunk service is a network connecting several central big ports, while a feeder service is focused on a single market characterized by a main port and a set of smaller ports. The model of this study can be applied to both types of service. The following paragraphs describes the features of a round service.

Value Proposition

The operative cost of the shipping company and the pollutants emitted have been considered to define a route in this study. They are two conflicting factors that lead to different solutions for the LRSOP. Indeed, when the operative cost are minimized, the vessel sails fast because it has to comply with the maximum transit times between ports. On the other hand, the vessel is going to slow steam when the pollutants are minimized. This does not mean that slow steaming is used only in the second case: sailing speed is optimized also in the first case because bunker cost is part of the operative cost. The considered pollutants are SO₂ and CO₂ and the external cost of emissions in USD is minimized in order to make the two objective functions comparable.

Frequency

The liner shipping industry differs from other maritime transportation modes primarily due to a fixed public schedule with a given frequency of port calls (Stopford, 2009). As the WestMed Service example in the introduction shows, a rotation with a weekly frequency is required in order to visit each port once a week. This goal is achieved by employing several vessels sailing once week apart. Rotation turnaround time varies from a single week up to 20 weeks. The sailing speed chosen during the rotation is strictly related to the number of vessels. Figure 2.7 depicts the relationship between number of vessels required and speed (in knots) for different service distances. It is clear that, given the total distance, more vessels have to be employed if the sailing speed decreases.

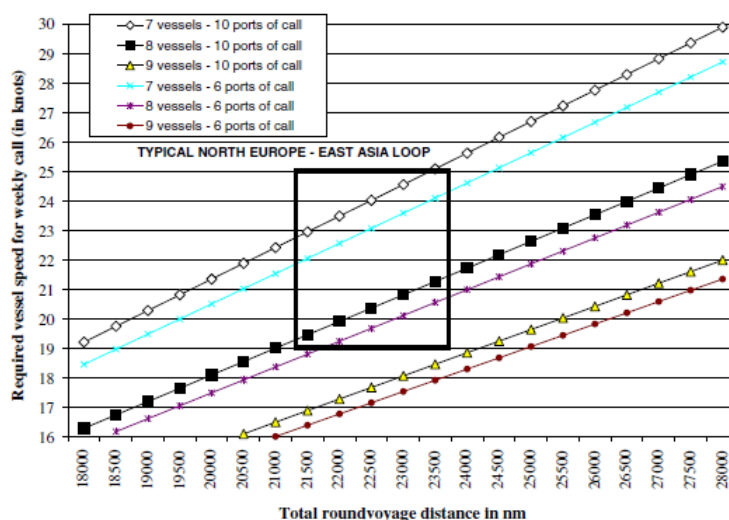


Figure 2.7: The relationship between roundtrip distance, required vessel speed and the number of employed vessels. (Notteboom and Vernimmen, 2009a)

There are some business rules that set a two-weeks frequency rotation for vessels with a capacity of at most 800 forty feet equivalent unit (FFE), or a four-weeks frequency for vessels with a capacity of at least 4200 FFE. Services using vessels with a capacity of at least 1200 FFE must have a weekly frequency.

Vessel

Container vessels are characterized by specifications as FFE capacity, weight capacity, maximum and minimum speeds, length, draft, number of reefer plugs and engine power. The defining attribute is FFE capacity given as a nominal number. Moreover, each vessel has a design speed and a design

fuel consumption at design speed. The vessel used in this study is Panamax 2400. Its features are shown in Chapter 4, Data Description.

Ports

Ports have a maximum draft, and the berths have a maximum length. This can provoke incompatibilities between ports and vessels. Feeder ports are usually small, main ports are bigger and have some transshipment facilities. The time spent in the port by a vessel, called port stay, depends on the amount of cargo to load and unload in the given port for that particular call. The ports considered in the instances of this study do not have incompatibilities with the vessel Panamax 2400.

Canal

The main canals traversed by marine shipments are the Panama canal and the Suez canal. They allow fast connections between continents and therefore they reduce operative costs. Vessels have to pay a transit duty. Panama canal has a draft limit, whereas Suez canal does not have draft restriction for container vessels. Canal costs are not considered in the mathematical model since it would increase the number of variables without any significant variation of the final solution.

Transit Time

Offering a short transit time is a competitive leverage for liner shipping companies. This is valid especially when goods have a high economic depreciation, like clothes, or they are perishable, like fruit. Maximum transit time between ports can also be affected by port rules or geographical necessities. Transit times restrictions are decisive for the final solution of the LSRSOP since generally the bunker cost savings are not enough to cover the cost of delays. Furthermore, it is very difficult to estimate this cost: a sensitive analysis of this value shows its impact on the final cost.

Bunker Consumption

Bunker consumption depends on the vessel type, the sailing speed, the draft of the vessel, the number of operational reefer containers powered by the vessel's engine, and the weather. Therefore estimating bunker consumption is not easy. As stated in Section 2.2, Formula 2.1 has been used in this study to base the bunker consumption estimation on the sailing speed. Since sailing speed and bunker consumption have a cubic relation, the relation between the sailing time and the bunker consumption will be the one shown in Figure 2.8. Indeed, when the transit time is high, the vessel burns less fuel and vice versa.

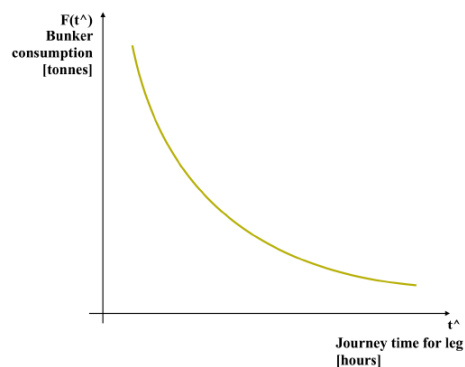


Figure 2.8: Sailing time-bunker consumption relation

Chapter 3

Literature Review

Liner Shipping Routing and Scheduling Problem is a sub-problem of Travelling Salesman Problem, the most studied problem in Operative Research (OR). Literature regarding routing and scheduling within liner shipping has doubled in the last decade; this means that it is a relevant and interesting research topic. Ronen (1983) wrote the first large overview that gives a classification of ship routing and scheduling problems and models. Liner shipping resembles a bus network as it publishes schedules and competes for cargo based on the service provided. Ronen points out that the analysis becomes more realistic if bunker consumption, the highest part of operating cost, depends on speed. Christiansen, Fagerholt, and Ronen (2004) and Christiansen, Fagerholt, Nygreen, et al. (2007) provide exausive surveys of OR in maritime transportation. They state that uncertainty takes an important role in maritime transportation and they hope to give the basis for future works. A detailed description of the Liner Shipping network is given by Brouer et al. (2013). They firstly give an overview of contributions of the LSNDP and then they provide a benchmark suite for developing future works. The model of Álvarez (2009) is extended and a column generation algorithm is used to solve it.

A useful contribution to solve large-scale instances of the Symmetric Traveling Salesman Problem (STSP) to optimality is given by Padberg et al. (1991). They took instances both from literature and from real cases; the algorithm is able to solve problems up to 2392 nodes. Kjeldsen (2011) provides a classification scheme for *routing and scheduling within liner shipping*. She shows that the model can have different formulations with respect to the final scope, cost structure, analysed variables and constraints. P. Alderton (1981) describes a variety of criteria to set the speed that maximizes profit. A model of liner shipping with non-simple routes is presented by Rana et al. (1991) but it does consider transshipments. The major liner shipping companies such as Maersk Line, MSC and Evergreen use weekly frequency for most of their services. The weekly frequency constraint is introduced by Fagerholt (2004) in the two stages approach to find the optimal solution of a liner shipping problem with weekly routes. In the first phase all the routes for each ship are generated, in the second phase an IP model minimize the total operational cost for the whole fleet. Agarwal et al. (2008) use the simultaneous ship-scheduling and cargo-routing model with weekly routes. The branch-and-cut method of Reinhardt and Pisinger (2012) and a MIP formulation of (Álvarez, 2009) solve smaller instances to optimality.

Managing the *time factor* is an important and, at the same time, challenging issue in liner service business. Delays due to port congestions, weather or waiting times before berthing or loading/unloading can have a negative impact on the companies profit (Notteboom, 2006). Algorithms to solve the TSP with time windows are described by Solomon (1987) and Baker (1983). As regard LSRSP, Fagerholt (2001) determines the optimal sailing speed in the so-called "soft-time window" model where penalties are imposed if the vessel do not respect the time windows. Hvattum et al. (2013) define the Speed Optimization Problem (SOP) and prove that, given the fuel consumption as a convex function of speed and a fixed sequence of port calls, each with time window, optimal speed can be found in quadratic time. Wang et al. (2012a) work on a robust schedule design problem using penalties for delays. The problem is a mixed-integer non-linear stochastic

model. Li et al. (2016) propose a multi-stage stochastic model in which legs are divided in segments and the final goal is to find the optimal speed on each segment. The SOP of Aydin et al. (2017) is characterized by stochastic port times and time windows. It is solved with dynamic optimization by discretizing port arrival times to find approximate solutions. An interesting conclusion is that real data from a liner shipping company performs better than data from benchmark methods.

The effect of bunker price on the network configuration of liner shipping has been studied by Stopford (2009) and Notteboom and Vernimmen (2009b). The latter state that managing *fuel consumption* gives the ship owner incentives to *slow steam*. Ronen (1982b) studies the fluctuation of oil price and how it affects the optimal speed. His analysis on the trade-off between fuel saving thanks to slow steaming and loss of revenue due to increase of travel time is relevant. The relationship between sailing speed and vessel size is studied in Ronen (2011). Lee et al. (2015) analyses the relationship among slow steaming, bunker cost and delivery reliability. A speed model that minimizes fuel consumption is presented by Du et al. (2011). They also define a non-linear and not necessarily cubic fuel consumption function.

In the recent years, the environmental impact of liner shipping has gained a lot of relevance. The above cited models can be extended by accounting the cost of *emissions* in the objective function. Psaraftis et al. (2013), Christiansen, Fagerholt, Nygreen, et al. (2013) and Meng et al. (2013) are the proof that liner shipping has focused not only on cost saving, but also on environmental issues. Psaraftis et al. (2013) provide a wide taxonomy of non-emissions speed models and emissions speed models. The study of Psaraftis et al. (2009) takes into account the SECAs, and shows that reducing emissions inside SECAs causes a speed increase outside to balance the transit time, with an overall emissions increase. Given a schedule sequence of port calls, each with time window, it is possible to adjust the speed on the legs in order to reduce emissions (Fagerholt, Laporte, et al., 2010). A big GHG reduction is achievable by optimizing sailing speed as well (Lindstad et al., 2011). They also argue that speed limits regulations are a possible way to reduce speed. Fagerholt, Gausel, et al. (2015b) show the effect of SECAs regulations; in particular, they analyse several scenarios where the vessels can choose different routes, inside and outside SECAs, to sail among ports.

Other relevant articles for this research are the ones related to *Biobjective Mixed Integer Programming*. The above cited Lindstad et al. (2011) use the Pareto Optimality approach to find solutions. Ehrgott et al. (2016) presents some of the theory for combinatorial optimization problems; Ehrgott (2006) and Eusébio et al. (2014) describe the ε -constraint method and how to find efficient solution on the Pareto Frontier with it. The Simulated Annealing Algorithm is well described in Bertsimas et al. (1993). Finally, Reinhardt, Clausen, et al. (2013) have been a good example of Simulated Annealing Analysis.

Chapter 4

Modeling

The proposed model to solve the Liner Shipping Routing and Speed Optimization Problem (LSRSOP) is described in this Chapter. In Section 4.1 the basic Travel Salesman Problem and the solution approaches are presented since the LSRSOP is based on it. As explained in Chapter 2, bunker cost and transit time have a cubic correlation (Brouer et al., 2013), therefore the Linearisation Method is required to measure the bunker consumption. The Linearisation Method of the Bunker Consumption Function is explained in Section 4.2. The description of the LSRSOP in words and its mathematical formulation are in Section 4.3. The proposed model to solve the LSRSOP is shown in Section 4.4. Two objective function can be used to define the rotation and the sailing speed among the ports: one that minimizes the pollutants emitted and one that minimizes the operative cost of the vessel.

4.1 The Traveing Salesman Problem

In the Asymmetric Travelling Salesman Problem (ATSP), the salesman has to visit all the cities minimizing the total distance in the round-trip configuration. There are many studies proving that the TSP is hard. Given a feasible solution, proving the optimality is difficult (Papadimitriou and Steiglitz, 1977). It is unlikely that there is a polynomial time algorithm to obtain an optimal solution. Indeed, if the number of cities increases, the number of variable increases exponentially. (Held et al., 1962) show that the number of cities permutations, i.e. all feasible routes, is $(N - 1)!$ for the ATSP.

The ATSP is defined on a *directed* graph $G = (V;A)$, where $V = \{1...n\}$ is the set of vertices and $A = \{(i, j)|i, j \in V\}$ is the set of directed arcs between the vertices. The ATSP is proven being *NP-hard* in Papadimitriou (1977). Given the distance between each pair of vertices $d_{(i,j)}, (i, j) \in A$, the basic ATSP formulation is the following:

Minimize:

$$\sum_{(i,j) \in A} d_{(i,j)} \cdot x_{(i,j)} \quad (4.1)$$

Subject to:

$$\sum_{j \in V} x_{(i,j)} = 1 \quad \forall i \in V \quad (4.2)$$

$$\sum_{i \in V} x_{(i,j)} = 1 \quad \forall j \in V \quad (4.3)$$

$$\text{the solution does not contain subtours} \quad (4.4)$$

$$x_{(i,j)} \in \{0, 1\} \quad \forall (i, j) \in V \quad (4.5)$$

The objective function 4.1 minimises the total travelled distance. If an arc (i, j) is in the final solution the boolean variable $x_{(i,j)}$ will be equal to 1. Constraints 4.2 and 4.3 ensure that only one arc leaves and enters each vertex and constraints 4.5 define the integrality of the decision variables. Constraints 4.4 avoid that the solution has more than 1 route and they are called in literature *subtour elimination constraints* (SEC). The number of these constraints can be extremely high and it strongly influences the running time to solve the problem. As Öncan et al. (2009) show, there are different formulations to apply these constraints, each one characterized by its number of generated constraints. Another issue to consider when the SEC are defined is the efficiency of them, i.e. how much they tighten the gap between the LP relaxation and the integer solution.

The LP relaxation is a technique that consists of replacing the integrality constraints of the variables with the constraint where each variable belong to the interval $[0,1]$. The LP relaxation produce, in case of minimization problems, a "lower bound" (LB), i.e. a feasible not-integer solution. Given two formulations of the same problem F1 and F2, we can say that F1 is stronger than F2 if the LB obtained from the LP relaxation of F1 is at least equal to the one obtained by solving the LP relaxation of F2. Once a formulation is chosen, it is necessary to choose the best strategy to fill the gap between the LB and the Optimal Solution (Figure 4.1).

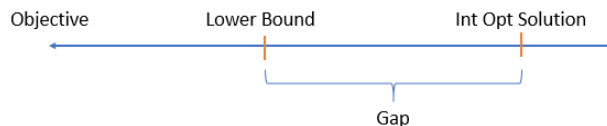


Figure 4.1: Gap between the Relaxed Solution and the Optimal Integer Solution

Among all the formulations for the SEC, two of them have been used in this study: the one proposed by Miller, Tucker and Zemlin (MTZ) and the one from Dantzig, Fulkerson and Johnson (DFJ). Given n vertices, the number of the SEC of the first formulation is polynomial while it is exponential for the second formulation; this means that the former has a lower computational complexity than the latter. On the other hand, DFJ's formulation is stronger than the MTZ's one in the LP relaxation (Öncan et al., 2009). MTZ constraints are part of the model proposed to solve the LRSOP and they are constraints 4.23 in Section 4.4; while DFJ constraints are used as explained in Section 6.4.1 and they are formulated as follows:

$$\sum_{i,j \in S} x_{(i,j)} \leq |S| - 1 \quad S \subseteq V, \quad 2 \leq |S| \leq n - 1,$$

where V is the set of all vertices, n is its cardinality and S any subset of V .

4.2 Linearization Method of the Bunker Consumption Function

One of the issues of modelling the LRSOP is how to calculate bunker consumption. As simple way to do it is suggested by Zis et al. (2016). The authors consider the specific fuel oil consumption of the engine, the engine load and the installed engine power. Obtaining these data for a specific vessel is sometimes hard and, even if the researcher has them, some approximations are required. Therefore, the Linearization Method of the Bunker Consumption Function has been used in this study as it is applied in other papers about liner shipping (Reinhardt, Plum, et al., 2016).

The cubic law 2.1 described by (Brouer et al., 2013) is a correct and accurate formula to relate the fuel consumption to the sailing speed variation. Given the distance between ports, the fuel consumption can be related to the transit time on the leg as well. The Linearization Method of the Bunker Consumption Function approximates the cubic relation between transit time and fuel consumption by using different secants as (Reinhardt, Plum, et al., 2016) shows in Figure 4.2. Of

course the more are the secants, the better the approximation will be. A linear static method has been chosen instead of a dynamic one in order to not make the model too much complex in computational point of view, allowing a small approximation. This method is well described in the thesis of Dithmer (2015).

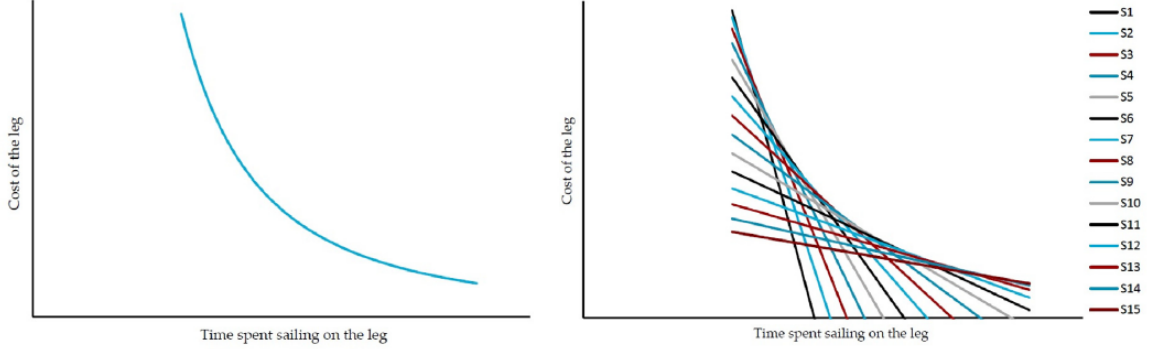


Figure 4.2: Fuel consumption in function of the sailing time (left); fuel consumption approximated by 15 secants (right)

Given the distance between two ports d and the design sailing speed s_* , the transit time on that leg at the design speed will be:

$$t_* = \frac{d}{s_*}. \quad (4.6)$$

By using the formula 4.6 in the cubic law 2.1, the bunker consumption can be written as follows:

$$\begin{aligned} F(t) &= \left(\frac{s}{s_*}\right)^3 \cdot f^* \\ &= \left(\frac{d/t}{d/t_*}\right)^3 \cdot f^* \\ &= t_*^3 \cdot \frac{1}{t^3} \cdot f^* \\ &= \left(\frac{d}{s_*}\right)^3 \cdot \frac{1}{t^3} \cdot f^* \\ &= \frac{f^*}{s_*^3} \cdot d^3 \cdot \frac{1}{t^3} \end{aligned} \quad (4.7)$$

The last equation 4.7 is the hourly bunker consumption for the vessel, when it takes time t to cover a given leg. Therefore, in order to obtain the total bunker consumption on that leg, the transit time t has to be multiplied to equation 4.7 obtaining:

$$F(t) = \frac{f^*}{s_*^3} \cdot d^3 \cdot t^{-2} \quad (4.8)$$

This is equation of the left function shown in Figure 4.2. As stated before, the secants are useful to approximate the cubic relation 4.8. Given a set of secants N and the transit time for each leg, we want to define their equation in order to compute the bunker consumption. The general formula to compute the bunker consumption y to changing transit time x is: $y = \phi x + \omega$, where ϕ is a negative slope and ω the intersection with the y -axis. The slope of secant n is:

$$\phi_n = \frac{F(t_n) - F(t_{n-1})}{t_n - t_{n-1}}; \quad (4.9)$$

the intersection of secant n is:

$$\omega_n = F(t_n) - \phi_n \cdot t_n; \quad (4.10)$$

where t_n is the end point of secant n and $F(t_n)$ the fuel consumption at time t_n . The journey time for the leg at each point t_n is equally spread across the interval $[t_0; t_N]$ that are the minimum and maximum transit times on the given leg. Given the distance between two ports i and j and N secants, the values of these transit times are:

$$t_0^{(i,j)} = \frac{d}{S_{max}} \quad \forall (i, j) \in A \quad (4.11)$$

$$t_N^{(i,j)} = \frac{d}{S_{min}} \quad \forall (i, j) \in A \quad (4.12)$$

$$t_n^{(i,j)} = \left(\frac{t_N^{(i,j)} - t_0^{(i,j)}}{N} \right) \cdot n + t_0^{(i,j)} \quad \forall (i, j) \in A, n \neq 0, N \quad (4.13)$$

The bunker consumption of secant n on leg (i, j) $BC_n^{(i,j)}$ is defined as equation 4.8:

$$BC_n^{(i,j)} = \frac{f^*}{s_*^3} \cdot d^3 \cdot (t_n^{(i,j)})^{-2} \quad \forall (i, j) \in A, n \in N \quad (4.14)$$

At this point it is possible to calculate the slopes ϕ_n and intersections ω_n for each leg as shown before:

$$\phi_n = \frac{BC(t_n^{(i,j)}) - BC(t_{n-1}^{(i,j)})}{t_n^{(i,j)} - t_{n-1}^{(i,j)}} \quad \forall (i, j) \in A, n = N \quad (4.15)$$

$$\phi_n = \frac{BC(t_{n+1}^{(i,j)}) - BC(t_n^{(i,j)})}{t_{n+1}^{(i,j)} - t_n^{(i,j)}} \quad \forall (i, j) \in A, n = 0, 1, \dots, N-1 \quad (4.16)$$

$$\omega = BC(t_n^{(i,j)}) - \phi_n \cdot t_n^{(i,j)} \quad \forall (i, j) \in A, n \in N \quad (4.17)$$

Equations 4.15, 4.16 and 4.17 are going to be used in the model to set the lower bounds of the bunker consumptions. In particular they are used in constraints 4.32, 4.33, 4.34, 4.35 in Section 4.4.

4.3 The Liner Shipping Routing and Speed Optimization Model

The Liner Shipping Routing and Speed Optimization Problem (LSRSOP) has the objective of **minimizing the bunker and the vessels leasing costs** while defining a feasible service among a set of ports. At the same time, the model can be used to find a rotation **minimizing the external cost of SO2 and CO2 emissions**. In particular, given:

- A set of ports, divided in ports inside the Sulphur Emission Control Areas (SECA) and ports outside the SECA;
- The legs between ports, divided in three sets: legs inside SECA, legs outside SECA, *crossing legs*, i.e. legs connecting 2 ports in different areas (from inside to outside SECA or vice versa) and legs that start and end inside SECA with a segment outside;
- The distances between the ports;
- The time the vessel stays in each port;

- A set of pairs of ports having a maximum transit time constraint;
- Maximum transit times between some ports;
- The percentage inside SECA for each leg;
- Slopes and Intersections of the bunker consumption/transit time graph (Section 6.2).

If a feasible solution exist, the *output* is:

- A rotation that visit each port once;
- The transit time between each pair of ports included in the best rotation;
- The number of vessels employed to guarantee a weekly frequency;
- The total bunker consumption on the rotation;
- CO2 and SO2 emissions;
- external cost of CO2 and SO2 emissions.

Hypothesis

Before explaining the mathematical model, it is important to point out the hypothesis of the model. These assumptions have been set in order to simplify the complexity of the model. The hypothesis are:

1. Sailing speed is supposed to be constant between ports; therefore the speed in the result will be considered as an average.
2. Canal cost is not considered in the objective function that minimizes the operative cost of the company since it would increase the number of variables without any significant variation of the final solution.
3. When the vessels enters and exits the ECA areas, the burnt fuel has to be changed and this operation takes approximately one hour and it is not considered in the model.
4. The maximum capacity of the vessel is not accounted in this study. The model considers the quantity transported, in Forty-foot Equivalent Unit (FFE), between some pairs of ports only to weight the hours of delay that can arise between these ports.

The following paragraphs will describe the mathematical formulation of the model to solve the LRSOP. Firstly, sets, parameters and variables are defined, then the objective functions and the constraints are explained in detail.

Sets and Parameters

As the ATSP has sets of vertices and arcs, the LRSOP has sets of ports and legs between them. Since the model takes into account the SECA, an additional partition of the ports and the legs has been needed. This allows the model to identify legs inside and outside SECA and the *crossing legs*. There is also a set for the pair of ports that have the maximum transit time. This is done in order to avoid unnecessary constraints with high false MTT values. Table 4.1 describes each set. Tables 4.2 and 4.3 show the parameters used in the model.

Table 4.1: LRSOP Sets

Set Name	Description
P	Set of all the ports
A	Set of all the legs
AE	Set of legs inside SECA
AN	Set of legs outside SECA
AC	Set of <i>crossing legs</i>
AM	Set of pair of ports that have a maximum transit time
Se	Set of secants to calculate the bunker consumption as shown in Section 4.2

Table 4.2: LRSOP Parameters

Parameter Name	Description	Domain	Unit of Measure
FCE	Fuel cost inside SECA	\mathbb{R}^+	[USD/ton]
FCN	Fuel cost outside SECA	\mathbb{R}^+	[USD/ton]
AV	Number of available vessels	\mathbb{Z}	[week] or [vessel]
TC	Market rate of a vessel called time charter rate (TC rate), i.e. cost of leasing a container vessel	\mathbb{R}^+	[USD/day·vessel]
t_i^{stay}	Time spent in the port i , $i \in P$	\mathbb{R}^+	[hours]
R	Cost per hour per FFE for not respecting the maximum transit time	\mathbb{R}^+	[USD/hour·FFE]
v_j^i	FFE, that is the quantity transported from port $i \in P$ to port $j \in P$	\mathbb{Z}	[FFE]
$MTT_{(i,j)}$	Maximum transit time between port i and port j , $(i, j) \in AM$	\mathbb{R}^+	[hours]
$l_{(i,j)}$	Distance between port i and port j , $(i, j) \in A$	\mathbb{R}^+	[nautical miles]
maxS	Maximum sailing speed of the vessel	\mathbb{R}^+	[nm/h]
minS	Minimum sailing speed of the vessel	\mathbb{R}^+	[nm/h]

Table 4.3: LRSOP Parameters 2

Parameter Name	Description	Domain	Unit of Measure
$segIn_{(i,j)}$	Percentage of the arc $(i, j) \in A$ inside SECA	\mathbb{R}^+	[1]
$\phi_{(i,j)}^p$	Slope of secant $p \in Se$ of arc $(i, j) \in AN$ or the segment of a crossing arc outside SECA	\mathbb{R}	[1]
$\phi_{(i,j)}^c$	Slope of secant $p \in Se$ of arc $(i, j) \in AE$ or the segment of a crossing arc inside SECA	\mathbb{R}	[1]
$\omega_{(i,j)}^p$	Intersection of secant $p \in Se$ with the y-axes of arc $(i, j) \in AN$ or the segment of a crossing arc outside SECA	\mathbb{R}^+	[1]
$\omega_{(i,j)}^c$	Intersection of secant $p \in Se$ with the y-axes of arc $(i, j) \in AE$ or the segment of a crossing arc inside SECA	\mathbb{R}^+	[1]

For an easier script of the model, it is possible to calculate the maximum $tt_{(i,j)}^{max}$ and minimum $tt_{(i,j)}^{min}$ transit time on each leg $(i, j) \in A$ as follows:

$$tt_{(i,j)}^{min} = \frac{l_{(i,j)}}{maxS}$$

$$tt_{(i,j)}^{max} = \frac{l_{(i,j)}}{minS}$$

Moreover, the parameters in Table 4.4 are required for the formulation that minimizes the pollutants emitted. The external cost of emission (MOVE, 2014) is taken into account in order to let the objective function have [USD] as unit of measure.

Table 4.4: LRSOP Emission Parameters

Parameter Name	Description	Domain	Unit of Measure
$CO2^{cost}$	External cost for CO2 emitted	\mathbb{R}^+	[USD/kg]
$SO2^{cost}$	External cost for SO2 emitted	\mathbb{R}^+	[USD/ton]
$CO2_E$	CO2 coefficient to compute the emission inside SECA	\mathbb{R}^+	[1]
$CO2_N$	CO2 coefficient to compute the emission outside SECA	\mathbb{R}^+	[1]
$SO2_E^{\%}$	Percentage content of SO2 into fuel used inside SECA	\mathbb{R}^+	[1]
$SO2_N^{\%}$	Percentage content of SO2 into fuel used outside SECA	\mathbb{R}^+	[1]

Variables

The time of arrival in each port is used to define the subtour elimination constraints. The arrival time of one random port is set to zero, meaning that it is the first and last port of the rotation. Like the ATSP, a binary variable define if a leg is in the final solution or not. The sailing speed can be derived by the transit time between ports. All the variables are described in Table 4.5.

Table 4.5: LRSOP Variables

Variable Name	Description	Domain	Unit of Measure
$x_{(i,j)}$	Binary variable that takes value 1 if the arc (i, j) is used in the solution	$x \in \{0, 1\}$	[1]
t_i	Time of arrival at port $i \in P$	\mathbb{R}^+	[hours]
$\tau_{(i,j)}$	Travel time on arc $(i, j) \in A$	\mathbb{R}^+	[hours]
$\tau_{(i,j)}^{c1}$	Travel time on the segment inside SECA of arc $(i, j) \in AC$	\mathbb{R}^+	[hours]
$\tau_{(i,j)}^{c2}$	Travel time on the segment outside SECA of arc $(i, j) \in CA$	\mathbb{R}^+	[hours]
f_j^i	Transit time from port $i \in P$ to port $j \in P$	\mathbb{R}^+	[hours]
d_j^i	Hours of delay from port $i \in P$ to port $j \in P$	\mathbb{R}^+	[hours]
$BCE_{(i,j)}$	Bunker consumption on arc $(i, j) \in AE$	\mathbb{R}^+	[tons]
$BCN_{(i,j)}$	Bunker consumption on arc $(i, j) \in AN$	\mathbb{R}^+	[tons]
$BCC1_{(i,j)}$	Bunker consumption on the segment <i>inside SECA</i> of the arc $(i, j) \in AC$	\mathbb{R}^+	[tons]
$BCC2_{(i,j)}$	Bunker consumption on the segment <i>outside SECA</i> of the arc $(i, j) \in AC$	\mathbb{R}^+	[tons]
S	Duration of the route	\mathbb{Z}	[weeks]

4.4 Mathematical Model for the LRSOP

It is possible to solve the LRSOP either minimizing the pollutants emitted cost or the operational cost of the vessel. The result of both the objective functions is the cost related to one vessel during the whole route. The route will lasts S weeks and S is the number of employed vessels to guarantee a weekly frequency to each port; see Section 1.1 for a further explanation.

The objective function 4.18 minimizes the pollutants emitted in the route. The bunker consumption is multiplied for the percentage of SO₂ contained into fuels and for a factor of 0.02 to obtain the SO₂ emitted. To compute the the CO₂ emitted, the bunker consumption is multiplied by a coefficient: CO_N for the fuel used outside the ECA and CO_E for the fuel burnt inside ECA (Psaraftis et al., 2013). Both values are then multiplied by the external cost of emissions MOVE

(2014) to have a final cost value in USD.

The objective function 4.19 minimizes the total operative cost. It includes four costs: bunker cost of the legs inside the SECA and the segment of the *crossing legs* inside SECA (first line), bunker cost of the legs outside the SECA and the segment of the *crossing legs* outside SECA (second line), the cost of delays (third line) and the cost for leasing the vessel (fourth line). FCE and FCN are the fuels costs [USD/ton] inside and outside SECA respectively since vessels has to use different fuels. Bunker consumptions of each leg BCE, BCN, BCC1, BCC2 [ton] are calculated in constrains 4.32, 4.33, 4.34, 4.35. Vessels leasing cost is given by multiplying the daily fee [USD/day · vessel], the number of weeks the route lasts and the number of days per week. Delays are allowed in the final solution because there are strict time restrictions between ports and, for some instances, it is not possible to meet all the maximum transit time constraints even if the vessel sails at the maximum speed. Three values are multiplied to obtain the penalty cost: the cost per hour per FFE for not respecting the maximum transit time [USD/hour·FFE], the variable that counts the hours of delay and the FFE transported. Finally, the total operative cost will be exactly the cost of the vessel during the route and it takes into account the cost of the delays between ports.

The two different objective functions and the constraints follow.

Minimize pollutants emitted cost:

$$\begin{aligned} & \left(SO_2^{cost} \cdot SO_E\% \cdot 0.02 + CO_2^{cost} \cdot CO_E \right) \cdot \left(\sum_{(i,j) \in AE} BCE_{(i,j)} + \sum_{(i,j) \in AC} BCC1_{(i,j)} \right) + \\ & \left(SO_2^{cost} \cdot SO_N\% \cdot 0.02 + CO_2^{cost} \cdot CO_N \right) \cdot \left(\sum_{(i,j) \in AN} BCN_{(i,j)} + \sum_{(i,j) \in AC} BCC2_{(i,j)} \right) \end{aligned} \quad (4.18)$$

or

Minimize operational cost:

$$\begin{aligned} & FCE \cdot \left(\sum_{(i,j) \in AE} BCE_{(i,j)} + \sum_{(i,j) \in AC} BCC1_{(i,j)} \right) + \\ & FCN \cdot \left(\sum_{(i,j) \in AN} BCN_{(i,j)} + \sum_{(i,j) \in AC} BCC2_{(i,j)} \right) + \\ & \sum_{i \in P} \sum_{j \in P} \left(R \cdot d_j^i \cdot v_j^i \right) + \\ & TC \cdot S \cdot 7 \end{aligned} \quad (4.19)$$

Subject to:

$$x(\delta^-(i)) = 1 \quad \forall i \in P \quad (4.20)$$

$$x(\delta^+(i)) = 1 \quad \forall i \in P \quad (4.21)$$

$$t_1 = 0 \quad (4.22)$$

$$t_j \geq t_i + t_i^{stay} + \tau_{(i,j)} - M1 \cdot (1 - x_{(i,j)}) \quad \forall (i,j) \in A \setminus \delta^-(1) \quad (4.23)$$

$$\sum_{(i,j) \in A} \tau_{(i,j)} + \sum_{i \in P} t_i^{stay} = 168 \cdot S \quad (4.24)$$

$$1 \leq S \leq AV \quad (4.25)$$

$$f_j^i - d_j^i \leq MTT_{(i,j)} \quad \forall (i,j) \in AM \quad (4.26)$$

$$f_k^i \geq f_j^i + t_j^{stay} + \tau_{(j,k)} - M1 \cdot (1 - x_{(j,k)}) \quad \forall (i,k) \in A, j \in P, i \neq k \quad (4.27)$$

$$x_{(i,j)} \cdot tt_{(i,j)}^{min} \leq \tau_{(i,j)} \leq x_{(i,j)} \cdot tt_{(i,j)}^{max} \quad \forall (i,j) \in A \setminus AC \quad (4.28)$$

$$x_{(i,j)} \cdot tt_{(i,j)}^{min} \cdot segIn_{(i,j)} \leq \tau_{(i,j)}^{c1} \leq x_{(i,j)} \cdot tt_{(i,j)}^{max} \cdot segIn_{(i,j)} \quad \forall (i,j) \in AC \quad (4.29)$$

$$x_{(i,j)} \cdot tt_{(i,j)}^{min} \cdot (1 - segIn_{(i,j)}) \leq \tau_{(i,j)}^{c2} \leq x_{(i,j)} \cdot tt_{(i,j)}^{max} \cdot (1 - segIn_{(i,j)}) \quad \forall (i,j) \in AC \quad (4.30)$$

$$\tau_{(i,j)} = \tau_{(i,j)}^{c1} + \tau_{(i,j)}^{c2} \quad \forall (i,j) \in AC \quad (4.31)$$

$$BCE_{(i,j)} \geq \phi c_{(i,j)}^p \cdot \tau_{(i,j)} + \omega c_{(i,j)}^p - M2 \cdot (1 - x_{(i,j)}) \quad \forall (i,j) \in AE, p \in Se \quad (4.32)$$

$$BCN_{(i,j)} \geq \phi^p_{(i,j)} \cdot \tau_{(i,j)} + \omega^p_{(i,j)} - M2 \cdot (1 - x_{(i,j)}) \quad \forall (i,j) \in AN, p \in Se \quad (4.33)$$

$$BCC1_{(i,j)} \geq \phi c_{(i,j)}^p \cdot \tau_{(i,j)}^{c1} + \omega c_{(i,j)}^p - M2 \cdot (1 - x_{(i,j)}) \quad \forall (i,j) \in AC, p \in Se \quad (4.34)$$

$$BCC2_{(i,j)} \geq \phi^p_{(i,j)} \cdot \tau_{(i,j)}^{c2} + \omega^p_{(i,j)} - M2 \cdot (1 - x_{(i,j)}) \quad \forall (i,j) \in AC, p \in Se \quad (4.35)$$

Constraints 4.20 and 4.21 ensure that all nodes have one outgoing and ingoing leg, where $\delta^+(i)$ and $\delta^-(i)$ denote the set of outgoing and ingoing legs of node i respectively. In other words, all the ports are visited once during the route. Constraints 4.23 are subtour elimination constraints ensuring that the tour connects all the ports in a single rotation. Given a leg (i,j) in the solution ($x_{(i,j)} = 1$), t_j time of arrival in j has to be greater or equal than the time of departure from i plus $\tau_{(i,j)}$ travelling time on the leg. If the leg is not in the solution, the constraint is not active thanks to $M1$. Constraint 4.22 sets ports 1 as starting port. Therefore, constraints 4.23 excludes ingoing arcs to port 1.

Constraint 4.24 enforces the rotation being a multiple of one week. S are the employed vessels and they are to be less the available ones, AV (constraint 4.25). As explained in Section 1.1, the number of weeks needed of the route coincides with the employed vessels, that is each port is visited once in each week.

Constraints 4.26 are maximum transit time constraints and they also give the value to the delays variables d_j^i . Transit time between each pair of ports f_j^i is calculated in constraints 4.27. The transit time from port i to port k has to be greater than the transit time from port i to port j , plus the time the vessel stays in j , plus the travel time from port j to port k . These constraints are not active when the arc (j,k) is not in the final route.

Constraints 4.28, 4.29, 4.30 set the travel times bounds, and therefore the sailing speed, according

to the maximum and minimum vessel speeds. Constraints 4.28 are referred to legs outside the SECAs; 4.29 and 4.30 limit the sailing speed in the *crossing legs* (set AC). Variables $\tau_{(i,j)}^{c1}$ and $\tau_{(i,j)}^{c2}$ are the transit times in the segment of the leg inside and outside the SECAs, respectively; then they are summed in constraints 4.31.

Constraints 4.32, 4.33, 4.34, 4.35 calculate the bunker consumption of the sets AE, AN and AC as explained in section 6.2.

The domains of the variables are shown in Table 4.5.

Big M

In general the Big-M notation is known for increasing the computational time of problems and, for this issue, it is always suggested to avoid it. As Williams (1999) explains, the Big-M value should always be as small as possible. The running time increases with a high Big-M because the lower bound decreases; therefore, the solver requires more time to "close" the gap between the integer optimal solution and the relaxed solution.

There are two Big-M in the model to "deactivate" the constraints when the leg is not in the solution. In particular, M1 has to be set to the largest value that the arrival time can take: $M1 = 168 \cdot AV$; it is used in constraints 4.23 and 4.27. M2 has to take the biggest value of the intersections in order to not account the bunker consumption if the leg is not in the solution (constraints 4.32 4.33 4.34 4.35). Indeed the slope values are going to be always multiplied for zero if the leg is not in the final route, thus the M2 has to be large enough to null the intersection value.

Chapter 5

Data Description

Data used as input to solve the model are described in this Chapter. A benchmark suite for liner shipping network design problems is provided by Brouer et al. (2013) and it is available on the web-site <http://www.linerlib.org/>. The benchmark has been defined by collecting real life data from Maersk Line. Almost all the data used in the tests come from this benchmark. During this study, three instances have been defined: 15 ports all around the world, 20 ports on the Atlantic Ocean and 10 American ports; they are going to be called [15Wor], [20Atl] and [10Ame] respectively.

Ports

For the first instance, 15 ports have been chosen to simulate a whole global network. Indeed, there are ports in North Europe, West and East US Coast and East Asia. Table 5.1 describes the ports with the name and location. It also shows the time spent in the port by the vessel; these values are not available in the benchmark cited above, therefore they have been generated randomly in a range between 15 and 25.

Table 5.1: World ports instance description

ID	UNLocode	Name	Country	Region	Port stay [hours]
1	BEANR	Antwerp	Belgium	Europe	17
2	GBFXT	Felixstowe	United Kingdom	UK	20
3	DEBRV	Bremerhaven	Germany	Europe	17
4	NLRMT	Rotterdam	Netherlands	Europe	17
5	FRLEH	Le Havre	France	Europe	19
6	USEWR	Newark	United States	US East Coast	20
7	USCHS	Charleston	United States	US East Coast	17
8	PAMIT	Manzanillo	Panama	US West Coast	17
9	USLAX	Los Angeles	United States	US West Coast	17
10	USOAK	Oakland	United States	US West Coast	24
11	JPTYO	Tokyo	Japan	Japan	17
12	JPUKB	Kobe	Japan	Japan	22
13	HKHKG	Hong Kong	Hong Kong	Hong Kong	20
14	TWKHH	Kaohsiung	Taiwan	Singa- pore	21
15	KRPUS	Busan	Korea	South Korea	18

Twenty ports in the Atlantic Ocean have been chosen for the second instance. Their descriptions are shown in Table 5.2. Like for the previous set of ports, the times spent in the ports have been generated randomly in a range between 15 and 25. This instance cannot be solved to optimality, therefore it has been resized to 10 ports, called [10Ame] in Chapter 6. These 10 ports are 1, 2, 4, 5, 7, 8, 9, 11 and 15 of Table 5.2. The third instance is made of American ports (Table 5.3).

Table 5.2: Atlantic ports instance description

ID	UNLocode	Name	Country	Region	Port stay [hours]
1	DEHAM	Hamburg	Germany	North Continent Europe	24
2	BEANR	Antwerp	Belgium	North Continent Europe	15
3	BRPNG	Paranagua	Brazil	Brazil	15
4	ITGIT	Gioia Tauro	Italy	West Med	21
5	NLRM	Rotterdam	Netherlands	North Continent Europe	20
6	USCHS	Charleston	United States	US East Coast	25
7	USMIA	Miami	United States	US Gulf Coast	23
8	USEWR	Newark	United States	US East Coast	17
9	GBFXT	Felixstowe	United Kingdom	UK	21
10	BRSSZ	Santos	Brazil	Brazil	21
11	CAMTR	Montreal	Canada	Canada East Coast	23
12	GHTKD	Takoradi	Ghana	West Africa	22
13	UYMVD	Montevideo	Uruguay	Brazil	17
14	ZADUR	Durban	South Africa	South Africa	16
15	MAPTM	Tangier	Morocco	West Med	21
16	ESALG	Algeciras	Spain	West Med	18
17	ESVLC	Valencia	Spain	West Med	15
18	MACAS	Casablanca	Morocco	West Med	21
19	AOLAD	Luanda	Angola	West Africa	22
20	BEZEE	Zeebrugge	Belgium	North Continent Europe	23

Table 5.3: American ports instance description

ID	UNLocode	Name	Country	Region	Port stay [hours]
1	PALB	Balboa	Panama	US West Coast	25
2	COBUN	Buenaventura	Colombia	South America West Coast	25
3	PECLL	Callao	Peru	South America West Coast	18
4	CLIQQ	Iquique	Chile	South America West Coast	22
5	PAMIT	Manzanillo	Panama	US West Coast	19
6	USLAX	Los Angeles	United States	US West Coast	17
7	USOAK	Oakland	United States	US West Coast	25
8	USEWR	Newark	United States	US East Coast	20
9	USCHS	Charleston	United States	US East Coast	19
10	USMIA	Miami	United States	US Gulf Coast	19

Vessel

The vessel used in this study is Panamax 2400. As its name says, vessels belonging to this class can sail across the Panama Canal and it has a maximum capacity of 2400 FFE. Its features -some of the parameters used in the tests- are described in Table 5.4. All the tests have been run considering 20 available vessels (parameter AV in Table 4.2).

Table 5.4: Panamax 2400

Feature	Value	Unit of Measure
Capacity	2400	[FFE]
TC rate	21000	[USD/day]
Draft	11	[m]
Min speed	12	[nm/h]
Max speed	22	[nm/h]
Design speed	16	[nm/h]
Bunker cons at design speed	57.4	[ton/day]

Bunker Cost

Data available in bunkerworld web-site (BunkerWorld, 2017) have been used to set the two bunker costs needed in the model. For the bunker cost inside SECA (FCE in the Table 4.4) the value of the "Maximum 0.1% Sulphur - Distillate Index", hereafter BW0.1%S Index, has been chosen. The value of the "BunkerWorld 380 Index", hereafter BWI380, has been set as the bunker cost outside SECA (FCN). Figure 5.1 shows the actual values of these fuel classes.

As stated on the web-site, the BWI380 is a weighted daily index made up of 20 key bunkering ports. To obtain a representative geographical spread, the ports were selected by size with reference to their geographical importance. Marine diesel oil (MDO) and marine gas oil (MGO) are included in the calculation of BWI.

About the BW0.1%S Index, it is a combined daily average dollar value index of distillate fuels that comply with the 2015 Emissions Control Area (ECA) sulphur limit. To obtain a representative geographical spread, the ports were selected by size with reference to their geographical importance.

In all the test shown in this reports, FCE takes value of 500 and FCN takes value of 320. Indeed, the more refined fuel is more expensive since it emits less sulphur than the cheaper does.



Figure 5.1: BW380 and BW0.1S cost (BunkerWorld, 2017)

Bunker Consumption

The Linearization Method (described in Section 4.2) of the bunker consumption function has been used to deal with the cubic relation between sailing speed and bunker consumption. In order to generate slopes and intersections of the diagram transit-time/consumption, 10 secants have been taken into account. Since the model has two different fuel prices for the two sea areas, two transit-time/consumption diagrams have been built: one for the inside SECA and one for the outside SECA. There is, indeed, a parameter that measures the percentage inside SECA of each leg: $segIn_{(i,j)}$, $(i,j) \in A$. Table 5.5 reports these values for the legs leaving Antwerp.

Table 5.5: Percentage of the leg inside SECA

from	to	%insideSECA
BEANR	BEANR	0
BEANR	GBFXT	1
BEANR	DEBRV	1
BEANR	NLRMT	1
BEANR	FRLEH	1
BEANR	USEWR	0,2
BEANR	USCHS	0,2
BEANR	PAMIT	0,1
BEANR	USLAX	0,1
BEANR	USOAK	0,1
BEANR	JPTYO	0,05
BEANR	JPUKB	0,05
BEANR	HKHKG	0,05
BEANR	TWKHH	0,05
BEANR	KRPUS	0,05

Thanks to this parameter, it is possible to calculate values of slope and intersection for both inside and outside SECA diagrams. *Slope* and *intersection* are the values of the transit-time/consumption diagram outside SECA, *slopeC* and *intersectionC* are the values of the transit-time/consumption diagram inside SECA. As expected, the values of the first diagram for the legs leaving Antwerp and going to another port in Europe are zero. Table 5.6 shows slopes and intersections values both for the inside and outside SECA diagrams for the first 8 secants from Antwerp (Belgium) to Newark

(US).

Table 5.6: Example of values to calculate the bunker consumption (see Section 4.2 for further explanations)

from	to	secant	slope	intersection	slopeC	intersectionC
BEANR	USEWR	0	-22,39	8581,61	-1432,79	17305,72
BEANR	USEWR	1	-19,11	7722,69	-1223,29	12353,11
BEANR	USEWR	2	-16,45	6986,62	-1052,73	11185,87
BEANR	USEWR	3	-14,26	6351,01	-912,47	10166,19
BEANR	USEWR	4	-12,44	5798,39	-796,06	9774,18
BEANR	USEWR	5	-10,92	5314,90	-698,64	8538,33
BEANR	USEWR	6	-9,63	4889,47	-616,49	7831,49
BEANR	USEWR	7	-8,54	4513,16	-546,74	7220,60

Emissions Cost

In order to compute the cost of emissions in the objective function 4.18, there is the need to calculate the tonnes of SO₂ and the kg of CO₂ emitted in the route. They both depend on the type of fuel used, therefore two different coefficient for each have to be used. The CO₂ coefficient to estimate the emissions has been set by IMO: a value of 3.1144 [kgCO₂/ton] for heavy fuel oil (outside SECA) and 3.206 [kgCO₂/ton] of gas/diesel oil fuel (inside). To compute the SO₂ emissions, the percentage of SO₂ content in the fuel has to be multiplied to the fuel consumption [ton] and an factor of 0.02, derived from the chemical reaction of sulphur with oxygen (Kontovas, 2014). In this study percentages of 0.1% and 3.5% have been chosen. As regard the external cost of emissions, MOVE (2014) provides the two values: 37 [USD/tonCO₂] and 12,700 [USD/tonSO₂].

Maximum Transit Time

Not all the pairs of ports have a maximum transit time, therefore constraints 4.26 and 4.27 are made only for a subset of A, called in the model AM. Some MTT values are shown in Table 5.7.

Quantity transported

Quantity transported is measured in Forty-foot Equivalent Unit (FFE). FFE is related to each pair of ports and it is useful in the operational cost objective function in order to weight the possible delay of the solution. Table 5.8 shows an exaple of quantity transported from Los Angeles.

Table 5.7: Example of MTT values

from	to	MTT [hours]	from	to	MTT [hours]
BEANR	DEBRV	264	USOAK	TWKHH	504
BEANR	USEWR	336	USOAK	KRPUS	552
GBFXT	PAMIT	480	HKHKG	BEANR	696
GBFXT	USLAX	888	HKHKG	GBFXT	768

Table 5.8: Example of quantity transported in FFE

from	to	FFE	from	to	FFE
USLAX	DEBRV	2	USLAX	HKHKG	319
USLAX	NLRTM	1	USLAX	TWKHH	231
USLAX	FRLEH	0	USLAX	KRPUS	380
USLAX	PAMIT	9	USLAX	PALBL	49

Chapter 6

Solution Methods and Results

This Chapter shows the methods used in this study to find the solution of the Liner Shipping Routing and Speed Optimization Problem (LSRSOP). The running time to find the optimal solution varies according the size of the instance as input. As explained in Section 4.1, the Travelling Salesman Problem is difficult to solve; moreover, the model defined to solve the LSRSOP adds additional constraints to the TSP making harder the computational complexity. Indeed, besides the well-known solving difficulties the subtour elimination constraints bring, the proposed model considers the maximum transit time constraints between some pairs of ports. The instances used in this analysis have been the ones described in Chapter 5; the 10 American ports, the 20 Atlantic ports and the 15 World ports instances will be denoted as [10Ame], [20Atl] and [15Wor] respectively. For the [20Atl] instance the 47% of pair of ports have a maximum transit time constraints while this percentage is 66 for the [15Wor]. This is one of the reasons why the solver takes a long time to solve the problem an it stops because a memory error occurs. Another reason is, of course, the number of ports, that determines the number of constraints. Indeed, while the percentage of the pairs of ports having a maximum transit time is 46% for the [10Ame] instance, the solver can find the optimal solution in 548.2 seconds. The [20Atl] instance have been downsized to 10 ports in order to have two instances that could be solved until optimality.

Therefore, according the above stated solving difficulties arisen from the instance as input, two solutions approaches have been implemented: the Optimal Solution approach and the Heuristic Approach. In the former, several techniques have been tested with the purpose of decreasing the overall running time; moreover, the Pareto Frontier of a Bi-Objective Functions Model can be found if the optimal solution is available. Instances used for these studies are the [10Ame] and the [10Atl] instances. The Heuristic Approach has the purpose of defining the best strategy to find a satisfying and feasible solution for the instances that would require too much running time to be solved until optimality, that are [20Atl] and [15Wor] in this study.

The program codes have been executed on the Hight Performance Computing (HPC) infrastructure of DTU. The maximum requested memory for each run is 46gb on one node with 9 processors per node (PPN). The code has been written in Julia for Mathematical Optimization (JuMP), a domain-specific modelling language for mathematical optimization embedded in Julia language; Gurobi was used as solver.

The Chapter is structured as follows. Section 6.1 introduces the heuristic techniques used in this study; Section 6.2 describes the 2-Steps Method and contains the Route Generation Algorithm, the Speed Optimization Model and the Hill-Climbing Algorithm. Results of the 2-Steps Method are in Section 6.2.4. Sections 6.3 describes the Simulated Annealing Algorithm and Section 6.3.1 shows how its parameters are tuned.

Section 6.4 describes and shows the result of all the techniques tested to help the solver in the research of the optimal solution. Results of the Bi-Objective function model are in Section 6.5.1;

these results are analysed both in the company and the environmental point of view. A Sensitive Analysis for the cost of delay was required to show the effect of this cost on the total operative cost of the vessel (Section 6.6). Finally, an As-Is/To-Be Analysis is presented in Section 6.7 to estimate the effect of the regulations issued by the International Maritime Organization (IMO) for the year 2020.

6.1 Heuristic Approach

The main issue for the LRSOP is finding the optimal port calls sequence that minimizes the objective function. Decreasing the complexing of the problem to obtain shorter running times is possible. Given a port calls sequence, i.e. a route, the model has to find the optimal sailing speed that minimizes the objective function; in this way, finding the best solution of the LRSOP is unlikely, but it possible to obtain a good feasible solution, not so far from the best one. Heuristic approaches are usually used by decision makers to find a feasible and satisfying solution of problems with an enormous number of possible solutions within a reasonable time. As regards the presented LRSOP, finding the best solution is hard for the solver when the operative cost of the shipping company is minimized, therefore the presented heuristic approaches are going to minimize the cited cost.

In this Section two heuristics are described and tuned in order to offer the best strategy to use with complex instances. The first heuristic proposed is the *Two-Steps Method* tries to improve the solution using the *Hill-Climbing Algorithm*, an algorithm that recombines the port calls to create a new route; the second is the *Simulated Annealing* that improves the solution allowing worse solutions if some condition are met in order to jump out any local optimums.

6.2 Two-Steps Method

The Two-Steps Method is inspired to the Two-Stages Approach used by Fagerholt (2004) to minimize the total operational cost. Hvattum et al. (2013) defined the Speed Optimization Problem (SOP) to find the optimal speed in quadratic time. The Two-Steps Method proposed in this study is composed as follows:

1. *Route Generation & SOP*: The Route Generation Algorithm proposes randomly different routes to the Speed Optimization Model; then, among all the routes, the one that best optimizes the SOP is chosen. Step 1 ends when the time limit is reached.
2. *Hill-Climbing & SOP*: Given the best solution of Step 1, the Hill-Climbing Algorithm generates a slight different route and the SOP evaluates whether it is better than the first one. This attempt can be made several times according to the time limit.

The 2-Steps can be repeated by setting a global time limit. The decision maker is going to choose this time limit according to the complexity of the problem and how much time he or she is willing to allocate for the search. Of course, the more time is used, the more solutions are going to be generated and improved.

In order to find the best 2-Step Method configuration, a single run has a global time limit of 5 minutes and the cycle Step 1 + Step 2 can be repeated more than once in the single run. Step 1 lasts 10 seconds and Step 2 improves the solution until the solver cannot propose better ones after 30 seconds. The number of the 2-Steps cycles in one test varies according to the efficiency of the Hill-Climbing Algorithm: the more improvements it generates, the more Step 2 lasts; for example, in the test of Figure 6.3 the 2-Steps cycle is repeated four times.

This algorithm is described in Section 6.2.3 and its best configuration is found in Section 6.2.4. The Route Generation Algorithm is described in Section 6.2.1 and the model to solve the Speed Optimization Problem (SOP) is in Section 6.2.2.

6.2.1 Routes Generation Algorithm

Algorithm 1 generates randomly different feasible routes. A route is feasible if all the ports are visited once and the travelled distance is viable at the maximum speed with the available vessels. This last hypothesis is important in order to ensure that the SOP does not optimize infeasible routes. The solution to deal with this issue is described in Section 6.2.3. The algorithm can be summarized as follows:

- Start from port 1 and add randomly other ports to the route until all the ports are visited;
- If the route has been already analysed from the Speed Optimization Algorithm, start the Algorithm from the beginning;
- If the route has not been analysed yet by the SOP, give this route as output and update the set of the analysed routes.

Inputs are the number of ports and the set of the routes already analysed in order to skip the SOP of routes already generated. This set is initialized as empty. The output is: an array of ordered ports, i.e. the rotation and the potentially updated set of analysed routes. The algorithm always starts to build the rotation from the port number 1, then each following port is chosen randomly between port 2 and the total number of ports. A boolean array called *visited_ports* keeps track of the ports already in the rotation. Once a no-analysed feasible route is found, the boolean values of $x_{(i,j)}$, $(i,j) \in A$ will be parameters in the SOP.

Algorithm 6.1: Routes Generation Algorithm

```

Data: { analysed_routes, #ports }
create a boolean array of visited ports visited_ports;
visited_ports[1] ← true;
cur_port ← 1;
create an array route with the port 1 as first element;
choose a random port j different from 1;
if the chosen port is not visited yet then
    | add this port to the array route;
    | cur_port ← j;
    | visited_ports[j] ← true;
end
already ← false;
if the route visits all the ports and it was already in the set analysed_routes then
    | already ← true;
end
if the route is not in analysed_routes then
    | add the route to analysed_routes;
end
if already = true then
    | start the algorithm from the beginning;
end
Result: { Feasible route,  $x_{(i,j)}$ ,  $(i,j) \in A$  values, analysed_routes }

```

6.2.2 Speed Optimization Problem

The SOP has basically the same formulation of the LRSOP but it does not have to find the best port calls sequence. Given a rotation, the SOP optimize the sailing speed minimizing the costs of the objective function. Since not all the legs have to be considered in the constraints, it is convenient resizing the sets in order to reduce the number of constraint (Table 6.1). The Big-M M2

is not necessary now since the constraints to measure the bunker consumption are created only for the used legs. On the other hand, the Big-M M1 is required only in constraints to calculate the transit times between ports (constraints 6.5) and it is activated by $x_{(i,j)}$, $(i,j) \in A$. Indeed, $x_{(i,j)}$ is a parameter in this model: it is equal to 1 if the arc (i,j) is in the rotation, 0 otherwise; its values are calculated looking at the port calls sequence of the input route. As regard variables, t_i , $i \in P$ are not needed any more since they were used only in the subtour elimination constraints (constraints 4.23). In addition to $x_{(i,j)}$, $(i,j) \in A$, the other parameters are the same of LSRSOP shown in Tables 4.2 and 4.3; Table 6.2 shows the variables of the SOP.

Table 6.1: SOP Sets

Set Name	Description
P	Set of all the ports
A	Set of all the legs
AE2s	Set of legs inside SECA
AN2s	Set of legs outside SECA
AC2s	Set of <i>crossing legs</i>
AM	Set of arcs that have a maximum transit time
Se	Set of secants to calculate the bunker consumption as shown in Section 4.2

Table 6.2: SOP Variables

Variable Name	Description	Domain	Unit of Measure
$\tau_{(i,j)}$	Travel time on arc $(i,j) \in A2s$	\mathbb{R}^+	[hours]
$\tau_{(i,j)}^{c1}$	Travel time on the segment inside SECA of arc $(i,j) \in AC2s$	\mathbb{R}^+	[hours]
$\tau_{(i,j)}^{c2}$	Travel time on the segment outside SECA of arc $(i,j) \in AC2s$	\mathbb{R}^+	[hours]
d_j^i	Hours of delay from port $i \in P$ to port $j \in P$	\mathbb{R}^+	[hours]
$BCE_{(i,j)}$	Bunker consumption on arc $(i,j) \in AE2s$	\mathbb{R}^+	[tons]
$BCN_{(i,j)}$	Bunker consumption on arc $(i,j) \in AN2s$	\mathbb{R}^+	[tons]
$BCC1_{(i,j)}$	Bunker consumption on the segment inside SECA of the arc $(i,j) \in A2sC$	\mathbb{R}^+	[tons]
$BCC2_{(i,j)}$	Bunker consumption on the segment outside SECA of the arc $(i,j) \in AC2s$	\mathbb{R}^+	[tons]
f_j^i	Transit time from port $i \in P$ to port $j \in P$	\mathbb{R}^+	[hours]
S	Duration of the route	\mathbb{Z}	[weeks]

Mathematical Formulation

For a detailed description of the objective function and the constraints see Section 4.3. The domains of the variables are shown in Table 6.2.

Minimize:

$$\begin{aligned}
& FCE \cdot \left(\sum_{(i,j) \in AE} BCE_{(i,j)} + \sum_{(i,j) \in AC} BCC1_{(i,j)} \right) + \\
& FCN \cdot \left(\sum_{(i,j) \in AN} BCN_{(i,j)} + \sum_{(i,j) \in AC} BCC2_{(i,j)} \right) + \\
& \sum_{i \in P} \sum_{j \in P} \left(R \cdot d_j^i \cdot v_j^i \right) + \\
& TC \cdot S \cdot 7
\end{aligned} \tag{6.1}$$

Subject to:

$$\sum_{(i,j) \in A2s} \tau_{(i,j)} + \sum_{i \in P} t_i^{stay} = 168 \cdot S \quad (6.2)$$

$$1 \leq S \leq AV \quad (6.3)$$

$$f_j^i - d_j^i \leq MTT_{(i,j)} \quad \forall (i,j) \in AM \quad (6.4)$$

$$f_k^i \geq f_j^i + t_j^{stay} + \tau_{(j,k)} - M1 \cdot (1 - x_{(j,k)}) \quad \forall (i,k) \in A, j \in P, i \neq k \quad (6.5)$$

$$tt_{(i,j)}^{min} \leq \tau_{(i,j)} \leq tt_{(i,j)}^{max} \quad \forall (i,j) \in AE2s \cup AN2s \quad (6.6)$$

$$tt_{(i,j)}^{min} \cdot segIn_{(i,j)} \leq \tau_{(i,j)}^{c1} \leq tt_{(i,j)}^{max} \cdot segIn_{(i,j)} \quad \forall (i,j) \in AC2s \quad (6.7)$$

$$tt_{(i,j)}^{min} \cdot (1 - segIn_{(i,j)}) \leq \tau_{(i,j)}^{c2} \leq tt_{(i,j)}^{max} \cdot (1 - segIn_{(i,j)}) \quad \forall (i,j) \in AC2s \quad (6.8)$$

$$\tau_{(i,j)} = \tau_{(i,j)}^{c1} + \tau_{(i,j)}^{c2} \quad \forall (i,j) \in AC2s \quad (6.9)$$

$$BCE_{(i,j)} \geq \phi_{(i,j)}^p \cdot \tau_{(i,j)} + \omega_{(i,j)}^p \quad \forall (i,j) \in AE2s, p \in Se \quad (6.10)$$

$$BCN_{(i,j)} \geq \phi_{(i,j)}^p \cdot \tau_{(i,j)} + \omega_{(i,j)}^p \quad \forall (i,j) \in AN, p \in Se \quad (6.11)$$

$$BCC1_{(i,j)} \geq \phi_{(i,j)}^p \cdot \tau_{(i,j)}^{c1} + \omega_{(i,j)}^p \quad \forall (i,j) \in AC2s, p \in Se \quad (6.12)$$

$$BCC2_{(i,j)} \geq \phi_{(i,j)}^p \cdot \tau_{(i,j)}^{c2} + \omega_{(i,j)}^p \quad \forall (i,j) \in AC2s, p \in Se \quad (6.13)$$

6.2.3 Hill-Climbing Algorithm

Once the best heuristic solution, among the routes generated in Step 1, has been selected from the SOP, it is possible to try to improve it with the Hill-Climbing Algorithm. The basic idea behind this algorithm is to switch some port calls in order to find a better and, in this case, cheaper solution. Figure 6.1 shows 2 similar routes. Route *b* is shorter than route *a* and it hopefully has a lower objective function value. The Hill-Climbing Algorithm tries to look for some good solution that the Routes Generation Algorithm did not proposed.

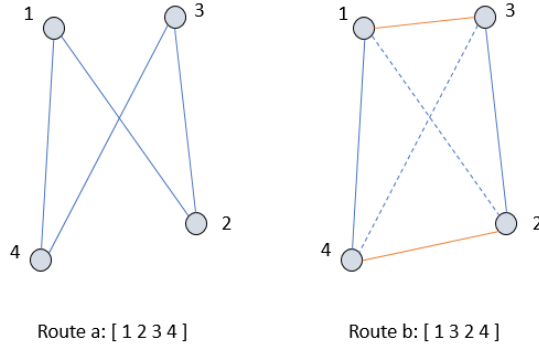


Figure 6.1: Length comparison between route a and route b

The classic approach of reverting a subsequence between two ports is not the best one for the presented problem, especially when the distances between the ports are very large. Indeed, it often generates routes that cannot be sailed with the maximum number of available vessels. For example, given the route [1,2,3,4,5,6,7,8,9,10] and reverting the ports between 3 and 8, the route [1,2,3,7,6,5,4,8,9,10] can result infeasible because, for example, if ports 3 and 4 belong to a continent and ports 7 and 8 belong to a different one, the total distance is too long. For this reason, the Algorithm proposed in this Section exchange the sequence of *at most* n ports. Figure 6.2 shows an example where only 3 of 4 ports are exchanged in the new generated route. Of course, the detailed-oriented reader is going to ask what is the maximum number of ports can be exchanged to maximize the efficiency of the algorithm. The answer to this question is in Section 6.2.4 where the results of the 2-Steps Method are shown.

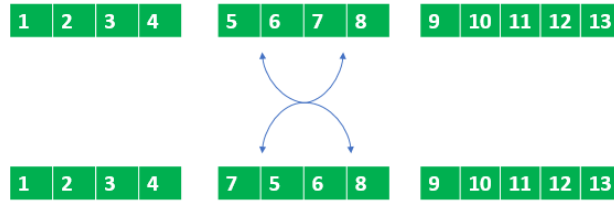


Figure 6.2: Example of Hill-Climbing Algorithm: given a maximum number of 4 ports exchanged, 3 of them are actually switched

Moreover, it is possible to calculate the maximum length of the route accessible with the available vessels. The number of the employed vessels in the rotation is equal to the number of weeks the rotation lasts in order to guarantee a weekly frequency to each port. Given the maximum sailing speed $maxS \left[\frac{nm}{h} \right]$, the available vessels $AV[weeks]$, the total time spend in ports $tot_stay[hours]$ and $168 \left[\frac{hours}{week} \right]$, the maximum accessible distance $AD[nautical\ miles]$ is calculated as follows:

$$AD = maxS \cdot (AV \cdot 168 - tot_stay) \tag{6.14}$$

The AD value is used in the Hill-Climbing algorithm and in the Routes Generation Algorithm to filter the the feasible rotation from the infeasible ones. In this way the efficiency of the study increase since the SOP does not have to analyse infeasible routes.

Before the detailed description of the Hill-Climbing Algorithm, it can be summarized in the next steps:

- Given a sequence of port calls, divide it in three parts;
- Mix randomly the order of the ports in the second part;
- Join the three parts in order to obtain a new route, different from the starting one;
- If the new route has been already analysed from the Speed Optimization Algorithm, start the algorithm again with the initial route;
- If the new route has not been analysed yet by the SOP, give this route as output and update the set of the analysed routes.

Algorithm 2 shows the Hill-Climbing Algorithm in detail. The input is the *best_route* among the ones generated from the Routes Generation Algorithm, the set of "improved" routes already tested called *tests*(initialized as empty) and the number of ports. In the shown description the output is a route with at most 4 switched port calls compared with the one as input and the updated set of the already tested routes; see next section for a deeper analysis. If the route has been already tested in the SOP, the algorithm generates a different new route starting from the one as input.

Algorithm 6.2: Hill-Climbing Algorithm

```
Data: {best_route, tests, #ports}
create an empty array mix;
n ← random(1:(#ports - 3));
i ← 0;
while i < 4 do
  | add the element in position best_route[n + i] to mix ;
  | i ← i + 1;
end
create an empty array end_route;
if best_route[n + 3] ≠ best_route[#ports] then
  | for i = (n + 4) : #ports do
  | | add the element in position best_route[i] to end_route;
  | end
end
create an array mix2 that has the same elements of mix in different order;
for i = n : #ports do
  | delete the last element of best_route;
end
append mix2 to best_route;
if best_route does not contain all the ports then
  | append end_route to best_route;
end
if best_route is in tests then
  | start again the algorithm with the initial route
else
  | add best_route to tests;
end
Result: {best_route, tests}
```

6.2.4 Two-Steps Method Results

Algorithm 2 breaks the rotation in three parts and changes the order of the ports of the second one, then the parts are linked again having a slight different rotation as output. The question is: *how many ports the second part should contain in order to maximize the efficiency of the algorithm?*

This section shows the result of the Two-Steps Method. In particular, it has been tested which one is the best Hill-Climbing configuration that finds best solutions. The method has the goal of finding different feasible solutions in order to achieve a good feasible solution. Two tests have been done: one on the [20Atl] instance and the second on the [15Wor] instance. Each test is composed of 5 runs; the single run lasts 5 minutes. It is possible that the cycle Step 1 + Step 2 is going to be repeated more than once in the single run. The first step, Route Generation Algorithm + SOP, looks for the best route among the ones generated for 10 seconds; the second step, Hill-Climbing Algorithm + SOP, improves the best solution of Step 1 until 30 seconds pass since the last SOP. In the Step 2 no SOP is run either the route is too long or the route proposed by the Hill-Climbing Algorithm has already been analysed. The run finishes, if, after Step 2, 5 minutes are passed from the beginning of the run.

Tables 6.3 and 6.4 report the result of the 2-Steps Algorithm for the [15Wor] and [20Atl] instances respectively. Three Hill-Climbing configurations are shown: when the algorithm changes the order of *at most* 4, 3 or 2 ports in the route. For both the instance the best configuration is when the algorithm exchanges at most 3 port calls. Indeed, the average of the tests is always the lowest for the 3 switch strategy. This result is highlighted especially in the instance of 20 ports. Finally, figure 6.3 shows an example of the 2-Steps run for the [15Wor] instance.

Table 6.3: 2-Steps Method result, instance: 15 World ports

Test	Best sol. 4 switch	Best sol. 3 switch	Best sol. 2 switch
1	241,592,681.05	240,098,749.76	241,218,289.84
2	213,188,812.90	214,499,885.15	245,766,752.17
3	256,124,083.77	245,732,501.10	205,315,511.94
4	292,239,636.83	233,245,682.93	225,402,870.38
5	214,359,651.16	229,423,919.95	250,980,207.57
Average	243,500,973.14	232,600,147.78	233,736,726.38
Std. D	32,811,909.21	11,903,910.93	18,542,192.03

Table 6.4: 2-Steps Method result, instance: 20 Atlantic ports

Test	Best sol. 4 switch	Best sol. 3 switch	Best sol. 2 switch
1	756,639,344.18	661,892,894.50	906,069,184.08
2	694,756,666.63	714,683,348.33	803,337,709.08
3	722,857,180.35	785,154,758.53	793,022,827.90
4	694,756,666.63	610,260,293.65	825,813,462.55
5	670,105,340.74	686,600,802.55	923,361,453.20
Average	707,823,039.70	691,718,419.51	850,320,927.36
Std. D	33,064,868.04	64,824,601.08	60,278,307.41

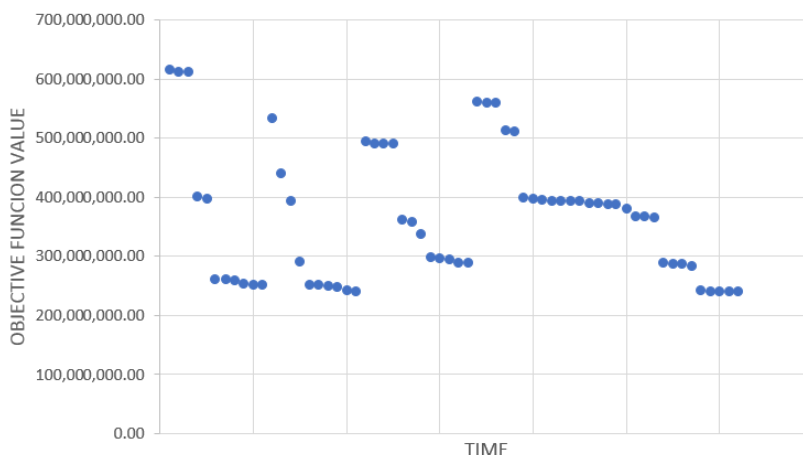


Figure 6.3: Example of 2-Step test for [15Wor] instance, maximum ports exchanged = 3; on the x-axis is the running time from 0 to 300 seconds.

6.3 Simulated Annealing

The Simulated Annealing technique, hereafter SA, is a meta-heuristic algorithm that consists of allowing the objective function to assume worse values in order to try to find a better value jumping out the local minimum. Aarts et al. (1988) prove that the algorithm can find an optimal solution with a high probability but the running time grows exponentially with the number of variables. The aim of this study is to tune the set of parameters in order to propose a good strategy to find a good solution for complex instances. The original meaning of annealing is the process of melting a metal with a high temperature and then bring it to the solid state again decreasing gradually and slowly the temperate. In optimization combinatorial problems, the algorithm starts from a given solution and then new configurations are analysed; the temperature has the key determinant role of deciding whether a worse solution has to be accepted or not. The lower the temperature, the less probability the new configuration has to be accepted. If the new configuration has a worse but similar solution from the current one, the probability of being accepted increases. Therefore, the algorithm works like a random search for high temperature and then it tries to go in depth looking for a good final solution with low temperatures. The difficulty of the method is the tuning phase because there are a lot of parameters to set and their variation can give very different results.

Given a starting solution x_0 with *energy* E_0 (its solution value), the initial temperature T^0 , the final temperature T^e and a *cooling rate* CR , the algorithm can be described with the following steps:

1. Generate a new solution x_1 starting from the current one with energy E_1 ; set $\Delta E = E_1 - E_0$;
2. If $\Delta E \leq 0$, the new configuration x_1 has a better solution than the current x_0 ; set x_1 as the current solution
3. If $\Delta E \geq 0$, the new configuration x_1 has a worse solution than the current x_0 ; generate a random number $p \in [0, 1]$; if $p \leq e^{-\frac{\Delta E}{T^0}}$, set x_1 as the current solution;
4. If the current temperature T^0 is equal to the final temperature T^e , end the algorithm; otherwise, update $T^0 = T^0 \cdot CR$ and continue from step 1.

6.3.1 Simulated Annealing Tuning

The SA has a lot of parameters to be tuned. Indeed, the result can vary enormously not only according to the running time, but also according the starting temperature and the cooling rate.

In this study, only the parameter to set the final temperature will be tuned; the Hill-Climbing Algorithm is used in the SA to find different routes that can have a worse or better solution value than the current one. The Hill-Climbing construction used for this heuristic approach is the 3-switched ports since it has been proven being better than the other constructions (Section 6.2.4). As it happens in the 2-Steps method, the routes generated from the Hill-Climbing algorithm having a length higher than AD nautical miles are not analysed by the SOP since they require more than 20 vessels (Section 6.2.3).

Since different instances are tested, the starting and final solutions have to be related by a law to compare the results. In this study, the running time links the two temperatures. Given the cooling rate CR and the running time α in seconds, the final temperature will be calculate as follows:

$$T^e = T^0 \cdot CR^\alpha \quad (6.15)$$

The CR can be calculated from 6.15 with the following formula:

$$CR = \left(\frac{T^e}{T^0} \right)^{\frac{1}{\alpha}} \quad (6.16)$$

The final temperature T^e is going to be a faction of the initial one and it will be tuned with the parameter \mathbf{r} :

$$T^e = T^0 \cdot r \quad (6.17)$$

The starting temperature T^0 has been set so that a solution $f\%$ worse than the starting one x_0 is going to be accepted with a probability of 50%. T^0 strongly influences the result according the running time. If the running time increases, f has to increase as well, otherwise, if it is too small, the SA is going to not accept any solutions for large part of the test. In this study, the running time of one test is 5 minutes and f has been set to 5% because it has been noticed that the SA works with this time/ f combination. Therefore, the equation to set the initial temperature will be:

$$T^0 = \frac{-0.05 \cdot x_0}{\log(0.5)} \quad (6.18)$$

The instances tested are the [20Atl] and the [15Wor]. Five tests have been run for each value of r ; each test lasts 5 minutes. Tables 6.5 and 6.6 show the best values for each test for both the instances. The result is that a value of $\mathbf{r} = 0.1$ brings better averages of solutions. Figure 6.4 is a test of when the parameter r is equal to 0.1 for the [15Wor] instance. Moreover, Figure 6.5 is a test of when the parameter r is equal to 0.001 for the [20Atl] instance.

Table 6.5: Best values of the tests of Simulated Annealing Analysis for 20 Atlantic ports instances; tuning the final temperature coefficient

	$\mathbf{r} = 0.001$	$\mathbf{r} = 0.01$	$\mathbf{r} = 0.1$
Test 1	994,463,227.02	968,102,324.40	1,007,717,067.46
Test 2	905,338,796.29	983,444,763.05	891,146,465.15
Test 3	965,581,427.51	1,021,296,018.47	882,389,950.85
Test 4	971,272,127.77	937,436,618.37	870,684,649.09
Test 5	978,776,650.24	930,636,094.90	970,314,792.54
Average	963,086,445.77	968,183,163.84	924,450,585.02
StD	34,054,024.22	36,773,056.43	60,839,686.56

Table 6.6: Best values of the tests of Simulated Annealing Analysis for 15 World ports instances; tuning the final temperature coefficient

	$r = 0.001$	$r = 0.01$	$r = 0.1$
Test 1	317,560,003.92	359,162,646.33	305,026,771.17
Test 2	337,236,648.43	386,887,989.00	266,896,581.67
Test 3	422,428,040.81	300,300,479.73	278,562,197.39
Test 4	294,312,886.57	298,613,208.15	335,520,848.00
Test 5	300,866,394.29	267,313,184.38	413,293,421.16
Average	334,480,794.80	322,455,501.52	319,859,963.88
St D	51,894,158.51	48,987,077.39	58,535,722.45

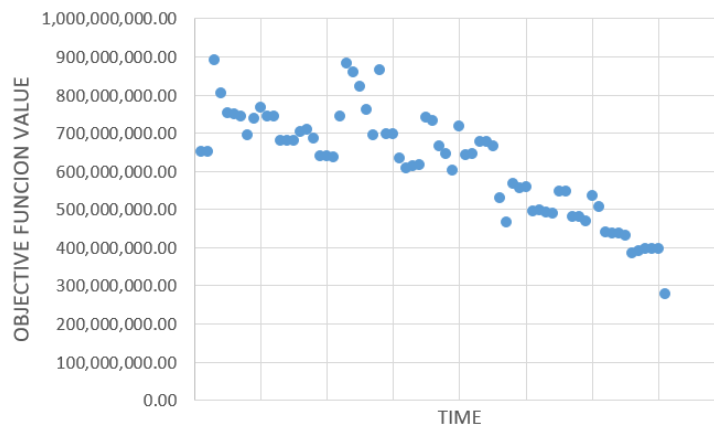


Figure 6.4: Example of SA test for [15Wor] instance, $r = 0.1$; on the x-axis is the running time from 0 to 300 seconds.

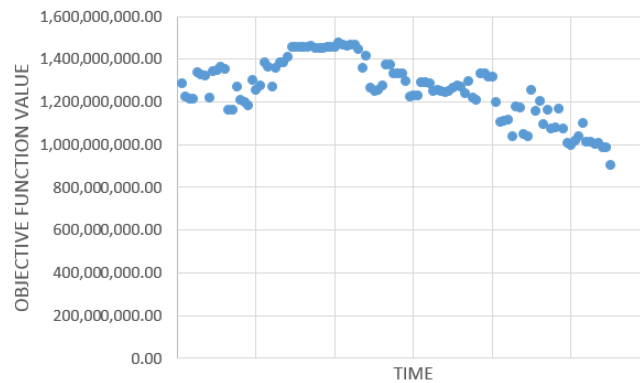


Figure 6.5: Example of SA test for [20Atl] instance, $r = 0.001$; on the x-axis is the running time from 0 to 300 seconds.

6.4 Optimal Solution

This section describes the techniques tested to find the optimal solution. Solving the problem until optimality is very hard in terms of both time and memory allocation. The formulation proposed has to deal with 2 issues: the number of *subtour elimination constraints* 4.22 and 4.23 and the *maximum transit times constraints* 4.26 and 4.27. It is possible to help the solver in finding the optimal solution by introducing dynamically inequalities, that means, adding to the model formulation new constraints if certain conditions are met while the branch-and-bound tree is explored. JuMP allows their addition by using *callback functions*. There are two types of these constraints: *Lazy Constraints* and *User Cuts*; in this study only the second type of constraints has been used. For the sake of completeness, the uses of Lazy Constraints and User Cuts are described before showing the tested User Cuts strategies.

A common and useful way to reduce the number of constraints is to remove the subtour elimination constraints and introduce them every time the MIP solver finds a subtour; these constraints are called "lazy". An example of solving the TSP with lazy constraints is provided by Iain Dunning and it is available on github (Dunning, 2013). Moreover, it is possible to use User Cuts to tighten the LP relaxation. Like lazy constraints, user cuts are introduced with a callback when a MIP solver reaches a new node in the branch-and-bound tree. The difference between user cuts and lazy constraints is that the former are not part of the original model and they are useful to eliminate a portion of the LP hull; the latter can remove a polygon where integer solutions are (Figure 6.6).

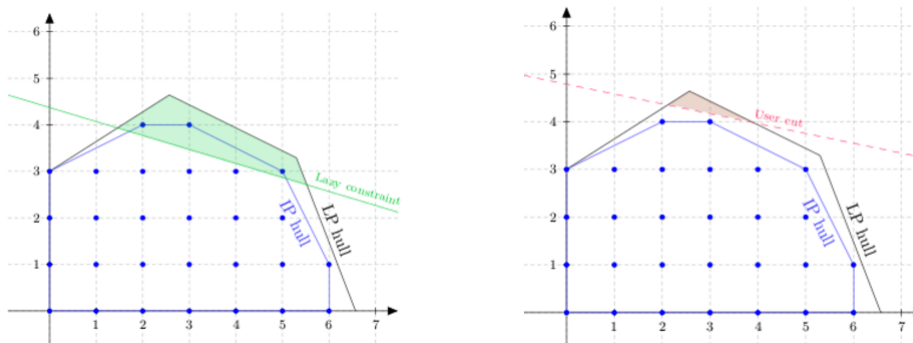


Figure 6.6: Use of lazy constraints and user cuts in an integer linear program

An algorithm that introduces subtour elimination constraints when the solution is still relaxed and that tightens the gap between the optimal and the relaxed solution is described in Section 6.4.1. Moreover other two types of user cuts have been tested to set lower bounds for the variables used in maximum transit time constraints. They are shown in Section 6.4.3. Unfortunately, they did not produce the expected improvements. The maximum flow algorithm has been tested with the purpose of decreasing the running time, but it has mediocre results.

6.4.1 User Cut: Subtours

The subtour elimination constraints (SEC) 4.22 and 4.23 introduced by Miller, Tucker and Zemlin (MTZ) produce a worse lower bound than the subtour elimination constraints proposed by Dantzig, Fulkerson and Johnson (DFJ) (Öncan et al., 2009). Figure 6.7 shows the known relationships between twenty-four ATSP formulations; indeed, among all the formulations, there are some proven being more efficient than others. Gavish and Graves (GG) is proven being better than MTZ, and DFJ is better than GG; therefore, it can be stated that DFJ is better than MTZ by transitive property. The drawback of the DFJ's formulation is that it creates an exponential number of constraints in comparison with the number of vertices. The number of MTZ's SEC is polynomial;

thus DFJ's formulation occupies much more memory and it takes more running time to solve the problem.

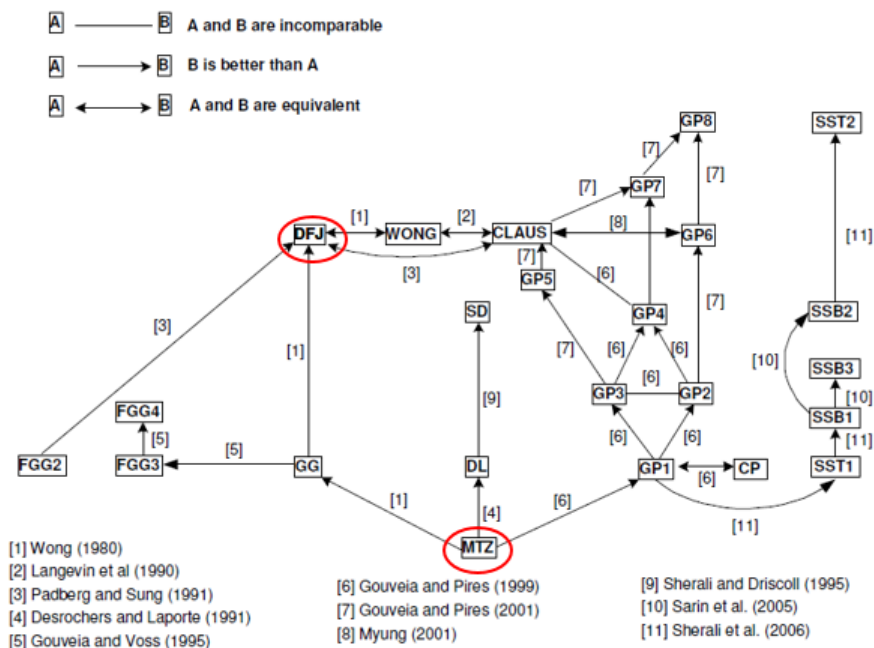


Figure 6.7: Known relationships between twenty-four ATSP formulations (Öncan et al., 2009)

Given a subtour S and n ports, $2 \leq |S| \leq n - 1$, the DFJ subtour elimination constraint has the following formulation:

$$\sum_{(i,j) \in S} x_{(i,j)} \leq |S| - 1 \tag{6.19}$$

While constraints 4.22 and 4.23 are still active, the proposed algorithm finds a subtour when the solution is relaxed and then it adds the DFJ constraint 6.19 as a user cut. In this way a portion of the LP hull is cut with the result of tightening the gap between the optimal integer solution and the LP relaxation.

Algorithm 3 shows all the steps to obtain a subtour starting from port 1. It can be summarized as follows:

1. Starting from port 1, look for all the connection between ports; a port i is connected to port j if $x_{(i,j)} \geq 0.001$
2. Every time a connection between port i and port j is found, update the outgoing (for port i) and ingoing (for port j) variables
3. For each port, add it to the subtour if both the outgoing and ingoing variables are greater or equal than 0.9

Figure 6.8 shows the first two subtours detected form the algorithm for the [10Ame] instance run. Since the algorithm starts looking for subtours from port 1, the user cuts introduced will be referred to the sets $[1, 8, 2, 3, 4, 7, 6]$ and $[1, 2, 8, 9, 5, 10]$. With regards to the first LP relaxed solution shown on the left, the following example shows how Algorithm 3 works until port 2:

1. Port 1 activates port 8; the ingoing and outgoing values are updated in this way:
 $outgoing_arcs[1] = 1, ingoing_arcs[8] = 1;$

2. Port 8 activates port 2; $outgoing_arcs[8] = 0.4633 + 0.5366$, $incoming_arcs[1] = 0.4633$, $incoming_arcs[2] = 0.5366$;

3. Port 2 activates port 3; $outgoing_arcs[2] = 0.5366 + 0.4633$, $incoming_arcs[1] = 0.4633 + 0.5366$, $incoming_arcs[3] = 0.4633$;

At this point the outgoing and ingoing values of ports 1 and 8 are greater than 0.9 and they will be added to the subtour in the end of the Algorithm. The Algorithm is described in detail in the rest of the Section.

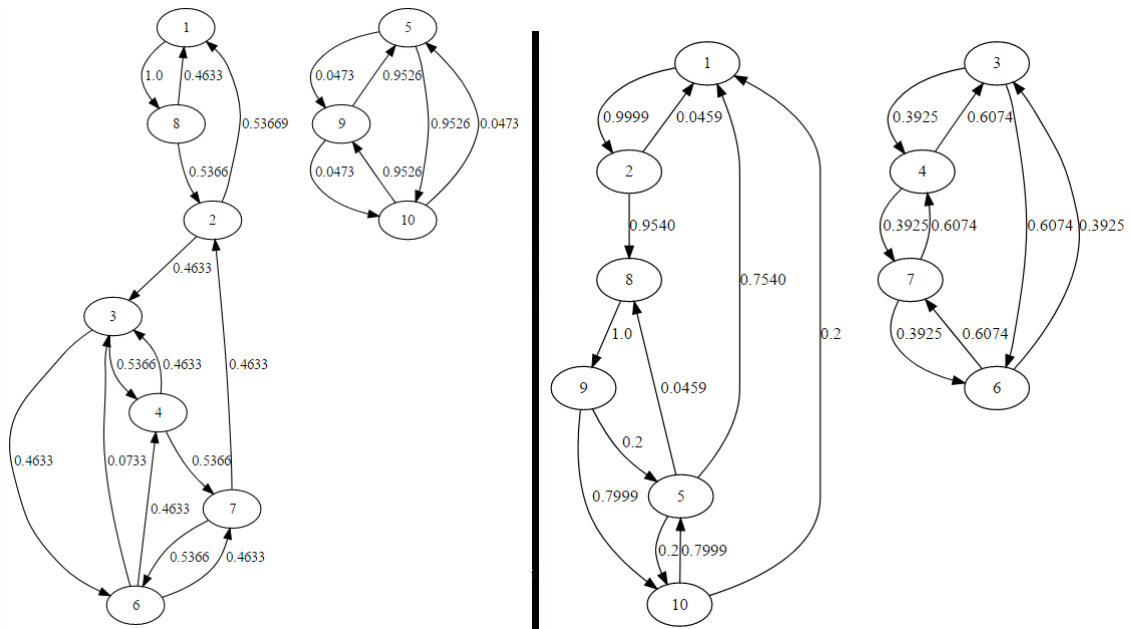


Figure 6.8: First (picture on the left) and second (picture on the right) subtours found from Algorithm 3 for [10Ame] instance run

The input data are the x values from the LP relaxation and the total number of ports. The output data are the number of ports in the subtour and an array that contains the ports in the subtour. Each port has an $incoming_arcs$ value and an $outgoing_arcs$ value; if, in the end of the algorithm, both of these values are higher than 0.9, the port is considered inside the subtour. The $visited_set$ set contain the visited ports and it is initialized having port 1. A port is active when one leg is connected with another active port. Then in one of the subsequent iterations, the algorithm finds the ports connected with the current active one and updates the respective $incoming_arcs$ and $outgoing_arcs$ values. Finally, an additional set $visited_set2$ is required in order to not update the set $visited_set$ while the first cycle "For" is still running. Once the subtour is found, the constraint 6.19 is added to the model. If the number of ports in the subtour is equal to the total number of the ports, no user cut is activated.

Algorithm 6.3: Subtours in LP Relaxation Algorithm

```

Data: {  $x_{(i,j)} \in R^+ \quad \forall(i,j) \in A, \#ports$  }
create arrays called ingoing_arcs, outgoing_arcs, subtour;
initialize port 1 as active port;
subtour_length  $\leftarrow$  0;
create a set visited_set and add 1 to it;
create a set visited_set2;
while do
  for  $i \in visited\_set$  do
    if i is an active port then
      for  $j = 1:\#ports$  do
        if  $x_{(i,j)} \geq 0.001$  then
          set port i as not active;
          ingoing_arcs[j]  $\leftarrow$  ingoing_arcs[j] +  $x_{(i,j)}$ ;
          outgoing_arcs[i]  $\leftarrow$  outgoing_arcs[i] +  $x_{(i,j)}$ ;
          if j is not in the set visited_set then
            add j to visited_set2;
          end
        end
      end
    end
  end
  add elements of visited_set2 to visited_set;
  if at least 1 port in visited_set is still active then
    continue;
  else
    stop the while cycle
  end
end
for each port i do
  if ingoing_arcs[i] > 0.9 and outgoing_arcs[i] > 0.9 then
    add i to subtour;
    subtour_length  $\leftarrow$  subtour_length + 1;
  end
end
Result: { subtour, subtour_length }

```

6.4.2 Subtour User Cut Result

As explained in the previous section, it is possible to use the subtours cuts to help the solver in tightening the gap between the optimal integer solution and the LP relaxation. In particular, this Section compare the running times of the MTZ's complete model (4.18-4.35) and the MTZ's complete model enriched by DFJ's User Cuts. The User Cut 6.19 is added when Algorithm 3 finds a subtour while the solution is still relaxed.

The comparison between the two formulations is made for [10Atl] and [10Ame] instances minimizing the operative cost because this is the worst case for the solver. For each instance and solving approaches, table 6.7 shows the lower bound of the first root, the gap between this lower bound and the final optimal solution and the total running time to obtain the optimal solution. Of course, both of the strategies bring to the same optimal solution. The result of this analysis is that the Subtour User Cut improves the efficiency of the formulation in the sense that the lower bound increases faster than the complete model with not user cuts. The problem is that the introduced

Table 6.7: Subtours User Cuts results compared with the complete model (4.18-4.35)

Instance	Subtour User Cuts	LB of the root node	Optimal solution value	Gap between root node LB and optimal solution	Running time [sec]
10 Atlantic ports	Yes	4,443,967.07	133,088,014.26	96.66%	1,375.92
	No	4,323,999.97	133,088,014.26	96.75%	502.25
10 American ports	Yes	1,963,312.52	5,344,065.36	63.26%	720.44
	No	1,850,643.56	5,344,065.36	65.37%	548.2

cuts increase the computational complexity and therefore the model takes more time to prove optimality.

Tables 6.8 and 6.9 show the optimal solution of [10Atl] and [10Ame] instances respectively in both the cases where operative costs and the external cost of emissions are minimized. Both of the total costs are related to one vessel during the whole route. The objective function that minimizes the operational costs of the shipping company is made of bunker cost, delays penalty cost and the cost of leasing the vessel. The two objective functions bring to definitely different solutions. Results for bigger instances, that are [20Atl] and [15Wor], are not reported since a memory error occurs before the solver finds the optimal solution.

As expected, when the cost of pollutants is minimized, the operative costs increase since the vessel sails as slow as possible in order to limit pollutants emissions. Indeed, bunker costs are consistently lower than the ones of the solutions that minimizes operative cost; the high operative cost is due to the fact there are penalties for the maximum transit times not respected. The bunker cost savings are not enough to cover the expenses for delays. This solution is unattainable because it is unlikely that the sailing company is going to make profit in this case. A *Bi-Objective model* is presented in Section 6.5 in order to find "golden line" solutions between the most convenient solution for the company and the most sustainable one in Section 6.5.

Table 6.8: Optimal solution for both the objective functions, instance: 10 American ports

	min: Operative cost	min: External cost of emissions
Route	[1 5 9 10 8 6 7 4 3 2]	[1 10 8 9 5 7 6 3 4 2]
Operative cost [USD]	5,344,065.36	13,481,012.18
Cost of emissions [USD]	28,953.54	8,076.43
Bunker cost [USD]	1,806,648.16	686,614.88
Penalty cost [USD]	2,655,417.20	11,177,397.30
Vessel cost [USD]	882,000.00	1,617,000.00
BC [ton]	4,809.19	1,700.98
CO2 emitted [kgCO2]	14,967.50	5,292.66
SO2 emitted [tonSO2]	2.24	0.62
CO2 emissin cost [USD]	553.80	195.83
SO2 emission cost [USD]	28,399.75	7,880.60
Weeks	6.00	11.00

Table 6.9: Optimal solution for both the objective functions, instance: 10 Atlantic ports

	min: Operative cost	min: External cost of emissions
Route	[1 7 4 2 10 8 5 6 9 3 1]	[1 7 2 8 6 5 9 3 10 4 1]
Operative cost [USD]	133,088,014.26	391,026,876.68
Cost of emissions [USD]	49,539.49	14,498.16
Bunker cost [USD]	3,629,877.89	3,052,576.68
Penalty cost [USD]	128,135,136.36	385,769,300.00
Vessel cost [USD]	1,323,000.00	2,205,000.00
BC [ton]	9,182.96	6,607.07
CO2 emitted [kgCO2]	28,960.60	21,069.63
SO2 emitted [tonSO2]	3.82	1.08
CO2 emissin cost [USD]	1,071.54	779.58
SO2 emission cost [USD]	48,467.94	13,718.58
Weeks	9.00	15.00

6.4.3 User Cuts: Lower Bounds for Delays and Transit Times

The Algorithm shown in this section has the goal of defining constraints that set lower bounds for the hours of delay $d_j^i, i, j \in P$ and transit times $f_j^i, i, j \in P$ variables. User Cuts 6.21 and 6.20 will be introduced, if all the conditions that will be defined in this Section are respected. Given a path between two ports, the transit time at the fastest speed is necessary to compute the minimum hours of delay. It is also possible that there is no delay between the two ports by sailing at the maximum speed. The transit time at the fastest speed includes the time spent in the ports of the path (parameters) and it is also the lower bound of the transit time variable between those two ports. On each node of the branch-and-bound tree, the algorithm tries to find useful bounds for the variables of each pair of ports with a maximum transit time constraint. The Algorithm to calculate the maximum delay and the minimum transit time can be summarized as follows:

1. Given a pair of ports with maximum transit time constraints (origin and destination), the Algorithm looks for the path with the highest $x_{(i,j)}, (i, j) \in A$ values between origin and destination;
2. If the path between origin and destination does not exist, stop the algorithm without adding any constraints;
3. If the path is found, update the variables output of the Algorithm, i.e. the minimum achievable transit time between origin and destination, the sum of the $x_{(i,j)}$ where (i,j) are the arcs linking the origin and destination, and the number of ports between them.

This paragraph describes in depth the Algorithm. Input of the algorithm are the $x_{(i,j)}, (i, j) \in A$ relaxed values (called $xStar$), the pair of ports (*from* and *to*), the parameters of the distances, the maximum sailing speed and the times in the ports. Moreover, the constraints that will be added have to be active only when the path between the two ports is used; therefore the x variables are another input in order to build an affine expression. For example, if the path from port 3 to port 2 is [3, 5, 15, 2], the relative affine expression will be: $x_{(3,5)} + x_{(5,15)} + x_{(15,2)}$.

A part from the affine expression aff_expr_x , the output will be the minimum hours of delay ($minT$) and the number of ports between *from* to *to*.

Algorithm 6.4: Lower Bounds for Delays and Transit Times Algorithm

Data: { from, to, xStar, $x_{(i,j)} \quad \forall (i,j) \in A$, dist, maxS, t_stay }

create the affine expression aff_expr_x ;
set the minimum transit time $minT$ to 0;
current \leftarrow from;
next \leftarrow 0;
 $x_value \leftarrow$ 0;
create the set *visited* and add *current* to it;
add $\leftarrow t_stay_{curr}$;
flow \leftarrow 0;
while do
 stop \leftarrow false;
 for $i \in P \setminus visited$ **do**
 if $xStar_{(curr,i)} \geq x_value + 0.01$ **then**
 add $\leftarrow \frac{dist_{curr,i}}{maxS} + t_stay_i$;
 $x_value \leftarrow xStar_{(curr,i)}$;
 next \leftarrow i;
 stop \leftarrow true;
 end
 end
 if stop = false and next \neq to or $x_value \leq 0.5$ **then**
 | stop the algorithm without adding any constraint;
 end
 $x_value \leftarrow$ 0;
 add next to *visited*;
 flow \leftarrow flow + $xStar_{(curr,next)}$;
 $aff_expr_x \leftarrow aff_expr_x + x_{(curr,next)}$;
 minT \leftarrow minT + add;
 if the path ends in the destination "to" and flow \geq (portsbetween + 0.001) **then**
 | end the algorithm and add the user cut;
 else
 | portsbetween \leftarrow portsbetween + 1;
 | current \leftarrow next;
 end
end
Result: { minT, aff_expr_x , portsbetween }

For each pair of port in the set AM (Table 4.1), the algorithm tries to find the path with highest x values among the pairs. The cycle *for* looks for the highest x value ($xStar$) starting from the port *from*. Once this value is found, the minimum transit time, the set of visited ports (*visited*), the value *flow* and the affine expression are updated. The cycle *while* is stopped if either there is no connection between the pair of ports or the x value is too low. The inequality will be activated only if the value *flow* is greater than the number of ports between the origin and the destination. The lower bound for the transit time variable will be:

$$f_j^i \geq minT \cdot (aff_expr_x - portsbetween) \quad (6.20)$$

As regard the lower bound for the delay variable, the constraint will be introduced if the minimum transit time is greater than the maximum transit time parameter $MTT_{(i,j)}$, $(i,j) \in AM$. The constraint introduced will be:

$$d_j^i \geq (\min T - MTT_{(i,j)}) \cdot (\text{aff_expr_x} - \text{portsbetween}) \quad (6.21)$$

Lower Bounds for Delays Result

Results of the Delay Penalty User Cuts are shown in this paragraph. If a path between two ports that have a maximum transit time constraint is found, the value of the affine expression is greater than the number of the ports between the origin and destination and the minimum transit time is greater than the transit limit, the cut 6.21 is introduced. Results for the [10Atl] and [10Ame] instances are provided in Table 6.10. The runs have been stopped after 3600 seconds. While the lower bound in the root node has a slight improvement than the one of the complete model when no user cut is added, it is interesting that the solution found for the [10Atl] instance is the optimal one, even if the gap is still large (93.1%).

Table 6.10: Maximum Delay User Cuts results compared with the complete model (4.18-4.35)

Instance	Max Delay User Cuts	LB of the root node	Best integer solution found	Gap between root node LB and optimal solution	Running time
10 Atlantic ports	Yes	4,390,639.80	133,088,014.26	96.70%	Time limit 1h, gap: 93.1% 502.25 sec
	No	4,323,999.97	133,088,014.26	96.75%	
10 American ports	Yes	1,863,302.74	5,424,486.20	65.13%	Time limit 1h, gap: 48.1% 548.2 sec
	No	1,850,643.56	5,344,065.36	65.37%	

Lower Bounds for Transit Times Result

Results of the Transit Times User Cuts are shown in this paragraph. Constraint 6.20 is introduced when the path between two ports having a maximum transit time is found and the value of the affine expression is greater than the number for the ports between the origin and the destination. Table 6.11 shows the results for the instance [10Atl] and [10Ame] instances; as for the test before, the running time has been stopped after 3600 seconds. Clearly, the running time using the two strategies of this section is longer than one using the Subtour User Cut.

Table 6.11: Transit Time User Cuts results compared with the complete model (4.18-4.35)

Instance	Transit Time User Cuts	LB of the root node	Best integer solution found	Gap between root node LB and optimal solution	Running time
10 Atlantic ports	Yes	4,394,733.83	133,088,014.26	96.69%	Time limit 1h, gap: 91.4% 502.25 sec
	No	4,323,999.97	133,088,014.26	96.75%	
10 American ports	Yes	1,863,302.74	5,424,486.20	65.13%	Time limit 1h, gap: 47.1% 548.2 sec
	No	1,850,643.56	5,344,065.36	65.37%	

Maximum Flow Algorithm

The Maximum Flow or Minimum Cuts Algorithm has been widely used to improve the running times of optimization problems. It was invented by Boykov and Kolmogorov and its application for graph problems is well explained by Stephan Diederich (Stephan Diederich, 2006). There is a predefined function in JuMP that allows the user to activate this algorithm. Unfortunately, the

Table 6.12: Maximum Flow User Cuts results compared with the complete model (4.18-4.35)

Instance	Subtour User Cuts	LB of the root node	Optimal solution value	Gap between root node LB and optimal solution	Running time [sec]
10 Atlantic ports	Yes	4,323,999.97	133,088,014.26	96.75%	Time limit 1h, gap: 72%
	No	4,323,999.97	133,088,014.26	96.75%	502.25
10 American ports	Yes	1,978,093.84	5,344,065.36	62.99%	3475.23
	No	1,850,643.56	5,344,065.36	65.37%	548.2

running time is not improved for the problem presented in this study. Indeed, the optimal solution for the [10Ame] instance is found in 3475.23 seconds and the [10Alt] instance seems to be complex to solve: the time limit stops the run after 1 hour. Also in this case, the solver finds the best solution soon, but it takes a long time to close the gap.

In conclusion, no one of the tested cuts applied to this problem decreases the running time.

6.5 Bi-Objective Function Model

It often happens that there are different conflicting objectives to consider while defining a good solution for real world problems. The problem described in Chapter 2 is an example where there are many goals that may influence the final strategy to put into practice. In this section a Bi-Objective Model is defined to consider both operative costs and pollutants emitted to solve the LRSROP. Given two objective functions, the number of optimal solutions is finite but large, and it grows exponentially with the number of the ports. The final aim is presenting a reasonable small set of solutions to the decision maker. This set has to offer a good range of solutions among all the *efficient solutions* to make the strategy selection easier. A solution is said efficient if its value corresponds to a *non-dominated point*. Before defining a non-dominated point, we firstly need to define a Bi-Objective problem. Formally, a Bi-Objective optimization problem can be defined as follows:

$$\min\{z(x) = Cx : Ax = b, x \in \{0, 1\}^n\} \quad (6.22)$$

where $x \in \{0, 1\}^n$ is a vector of n binary variables; C is the cost matrix $\mathbb{Z}^{p \times n}$ with $p = 1, 2$ objective functions and $A \in \mathbb{Z}^{m \times n}$, $b \in \mathbb{Z}^m$ are the matrix and vector to define the m constraints. The set $Y = z(X) = \{Cx : x \in X\}$ is the feasible set in objective space \mathbb{R}^p . It defines the hull region called Edgeworth-Pareto, shown in Figure 6.9 (Ehrgott et al., 2016). A solution $x^* \in X$ is *efficient* if there is no $x \in X$ such that $Cx \leq Cx^*$ and its corresponding point $y^* = Cx^*$ is said *non-dominated*. Point y dominates y' if $y \leq y'$ and $y \neq y'$, that is, $y_p \leq y'_p$ for $p = 1, 2$ with at least one strict inequality. All the non-dominated points define the so called Pareto Frontier, i.e. the set of optimal solutions for the bi-objective model. A solution $x' \in X$ is *weakly efficient* if there is no $x \in X$ such that $Cx < Cx'$ Eusébio et al. (2014). Points (9,1) and (1,9) are weakly non-dominated points because they both belong to the Pareto Frontier but there are better non-dominated points, (7,1) and (1,8) respectively.

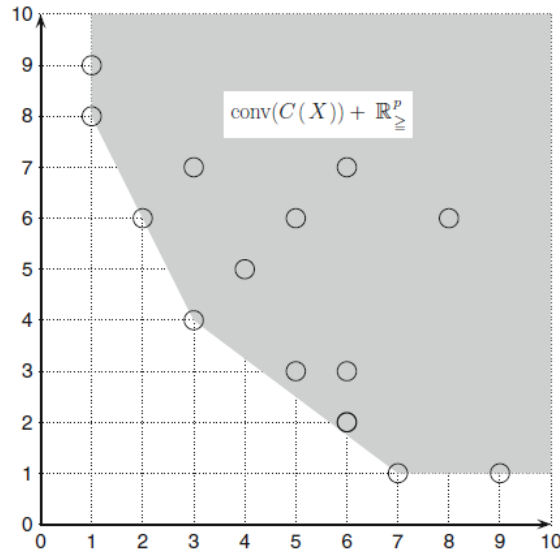


Figure 6.9: Edgeworth-Pareto hull (Ehrgott et al., 2016)

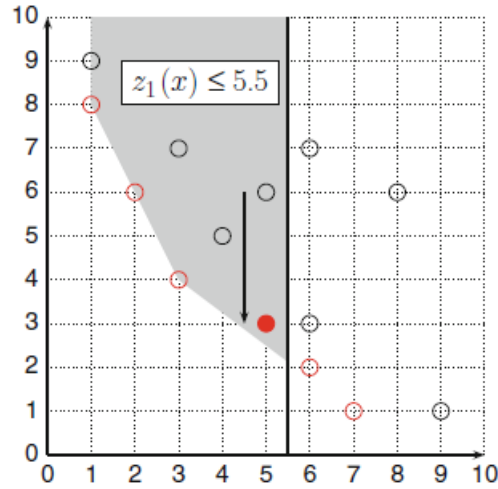
As regard the complexity of the bi-objective model, it is obvious that, since the single LRSOP is NP-hard, the bi-objective version of the LRSOP is also NP-hard. There are several algorithms to solve a multi-objective problem; in this study the *scalarization* technique has been chosen. The scalarization consists of solving repeatedly a single objective problem with additional constraints to find efficient solutions.

The ϵ -constraint method

The ϵ -constraint method is a scalarization algorithm that allow to find all the efficient solutions with appropriate parameters. This is a very good property that the Weighted Sum method does not have. The drawback of the the ϵ -constraint method is that it changes the structure of the problem by adding constraints, making the problem harder to solve (Ehrgott et al., 2016). The ϵ -constraint algorithm is described in this section.

Given two objective functions $z_1(x)$ and $z_2(x)$ and m constraints $Ax = b$ as they were defined above, the goal is finding points of the Pareto Frontier. Saying ϵ is the solution of $\min\{z_1(x)\}$, this corresponds probably to weakly non-dominated point. Therefore, the problem 6.23 is solved to find an efficient solution. In general, every time a point is found, there is the need to check whether it is dominated by another point. Figure 6.10 is an example where $\epsilon = 5.5$. The stating feasible solution is dominated by the one visualized with a red point.

$$\begin{aligned}
 &\text{minimize} && z_2(x) \\
 &\text{subject to:} && Ax = b \\
 &&& z_1(x) \leq \epsilon
 \end{aligned} \tag{6.23}$$

Figure 6.10: The ϵ -constraint method scalarization (Ehrgott et al., 2016)

Algorithm 5 shows how it is possible to find 3 points on the Pareto Frontier of a Bi-Objective model. The input are the two objective functions and the constraints of the problem. Once 2 optimal solutions are found, it is possible to find a third point -if it exists- having the solution values included in the ranges of the two points. This is made by setting the middle point of one of the objective function values less than ϵ . The algorithm can continue in this way to find other optimal solutions. In order to deal with tolerances of the solver, a small number is always added to the ϵ , e.g. 0.001.

Algorithm 6.5: Non-dominated points on the Pareto Frontier research

Data: { Objective functions $z_1(x)$ $z_2(x)$ }
 find solution ϵ minimizing OF $z_1(x)$;
 find point $\{x_1, y_1\}$ minimizing OF $z_2(x)$ and having $z_1(x) \leq \epsilon$;
 find solution ϵ minimizing OF $z_2(x)$;
 find point $\{x_2, y_2\}$ minimizing OF $z_1(x)$ and having $z_2(x) \leq \epsilon$;
 set a middle point as $\epsilon = \frac{x_1 + x_2}{2}$;
 find point $\{x_3, y_3\}$ minimizing OF $z_2(x)$ and having $z_1(x) \leq \epsilon$;
 check that $\{x_3, y_3\}$ is non-dominated minimizing OF $z_1(x)$ and having $z_2(x) \leq y_3$;
Result: $\{\{x_1, y_1\}, \{x_2, y_2\}, \{x_3, y_3\}\}$

6.5.1 Bi-Objective Model Result

This section shows the result of the Bi-Objective function model analysis for the [10Ame] instance. After the description of the points belonging to the Pareto Frontier a cost analysis is done for both the company and the environmental points of view.

Every time a point of the Edgeworth-Pareto hull is found by minimizing one OF, it has to be checked whether it is dominated by minimizing the other OF. Table 6.13 shows 5 dominated and non-dominated points. For example, the Point 6 (8,269,609.76 ; 8,521.5) dominates the optimal

solution of the Environmental point of view (Point 6 domin.). In those solutions the pollutants emitted costs have almost the same value, but then the operational cost are minimized obtaining a value of 8.269 Million[USD] instead of 9.403 Million[USD]. This is the proof that the Bi-Objective model is a powerful tool to balance more conflicting factors that influence the final decision.

Figure 6.11 depicts 8 efficient solutions; their values are shown in Table 6.14. Points 3 and 4 have similar solution values, but they are both efficient solutions.

Table 6.13: Bi-Objective Model Result, example of dominate points, instance: 10 American Ports

Point:	Operative cost [USD]	External cost of emissions [USD]
Point 1 domin.	5,344,065.36	28,953.54
Point 1	5,344,065.46	28,953.51
Point 8 domin.	13,481,012.18	8,076.43
Point 8	13,463,742.98	8,076.53
Point 6 domin.	9,403,904.32	8,521.42
Point 6	8,269,609.76	8,521.52
Point 7 domin.	10,866,676.47	8,394.73
Point 7	10,085,004.14	8,394.83
Point 5 domin.	6,806,837.71	11,225.05
Point 5	6,806,824.72	11,225.05

Table 6.14: Bi-Objective function model result, instance: 20 Atlantic Ports

Point of graph in Figure 6.14	Operative cost [USD]	External cost of emissions [USD]
Point 1	5,344,065.46	28,953.51
Point 2	5,569,305.36	26,879.82
Point 3	6,040,498.82	15,518.63
Point 4	6,279,490.57	15,352.33
Point 5	6,806,824.72	11,225.05
Point 6	8,269,609.76	8,521.52
Point 7	10,085,004.14	8,394.83
Point 8	13,463,742.98	8,076.53

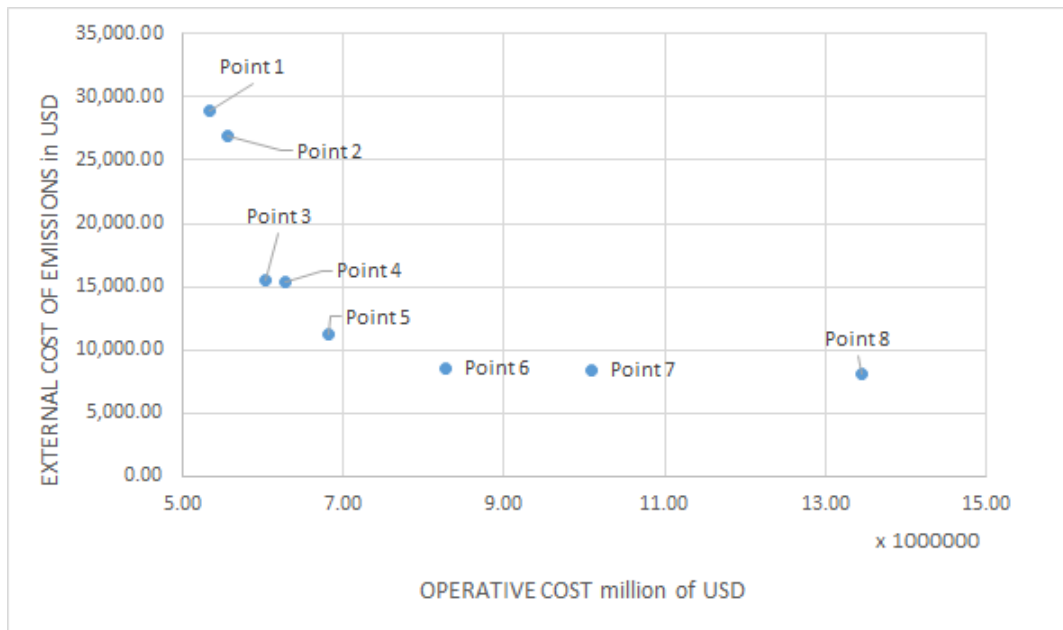


Figure 6.11: Bi-Objective function model Result: Pareto frontier of 10 American Ports

6.5.2 The shipping company point of view

It is interesting at this point making a comparison between the solutions on the Pareto Frontier. Figure 6.12 shows the average sailing speed of the 8 solutions. The average speeds of the first two points are very high because those points minimize especially the operative cost of the vessel. The solution of Point 2 has a slight higher average speed than the one of Point 1, indeed the bunker consumptions of these solutions are 4,874.04 and 4,809.19 ton respectively. The average speed decreases in solutions where emissions are less. When the operative cost is minimized, the vessel has to sail fast in order to decrease the cost of delays. The advantage for the company when the speed is optimized is the bunker cost saving. Indeed, as Table 6.15 shows, the bunker cost is less and less when a "slow-sailing" solution is chosen. On the other hand, the cost of non-respected transit times represents a consistent part of the total cost and the bunker consumption savings are not enough to cover the expense for delays (Table 6.15). Moreover the slower-sailing solutions last 2 or 3 weeks more, therefore the cost for leasing the vessel increases as well. However, Points 7 and 8 are the proof of that, even if the bunker cost have small changes, the company can obtain high cost savings changing the rotation in order to respect some maximum transit times. The rotations for these solutions are consistently different, that is why the Operative Research can give a consistent contribution to the management of shipping companies.

The operative cost of the company strongly depends on the cost per hour of delay. The *sensitive analysis* of this value is interesting in order to calculate the operative cost variation. In general, the cost of non-respected transit times is high for perishable goods. However, estimating its value is very difficult since the vessel transports a lot of different goods. A value of 100 [USD/h·*FFE*] has been estimated for the result shown until now. The results of the sensitive analysis of the delay cost are reported in Section 6.6.

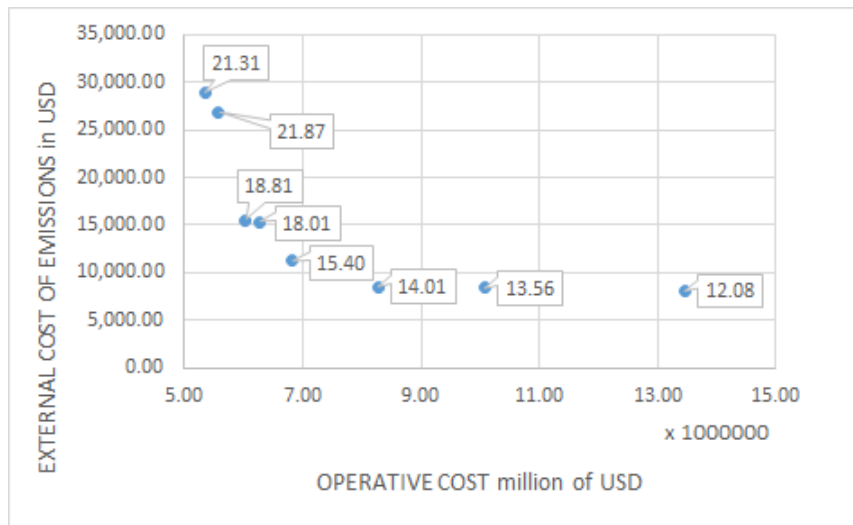


Figure 6.12: Average sailing speeds in Knots for the solutions on the Pareto Frontier

Table 6.15: Bunker and delay penalty costs for the solutions on the Pareto Frontier

Point of graph in Figure 6.14	Bunker cost [USD]	Delay penalty cost [USD]
Point 1	1,806,648.93	2,655,416.53
Point 2	1,885,224.41	2,802,080.96
Point 3	1,475,078.95	3,536,419.87
Point 4	1,488,393.46	3,762,097.11
Point 5	1,169,130.46	4,461,694.26
Point 6	827,140.76	6,119,469.00
Point 7	957,690.07	7,657,314.07
Point 8	686,750.32	11,159,992.66

6.5.3 The environmental point of view

As regards pollutants emitted, Table 6.16 shows the amount of CO₂ and SO₂ emitted for each point of the Pareto Frontier. Since, in general, the average sailing speed decreases from Point 1 to point 8, the vessel burns less fuel and therefore emissions decrease. Figures 6.13 and 6.14 compare the most convenient solution for the company and the other efficient ones. They show the quantity of pollutants savings of the efficient solutions compared with the company best alternative, and they also report the percentage of cost increment the company is going to pay whether it chooses a different solution from its best one. Slow steaming strategy has positive result for the environmental point of view. Indeed, saving of CO₂ and SO₂ emissions are relevant (25.69% and 46.81%) if the solution of Point 3 is chosen instead of the one corresponding to Point 1. Again,

the cost of the delay strongly influences the final decision. Given a cost of 100 dollars per hour of delay, the company is supposed to pay 13.03% to choose the solution of Point 3 instead of the one of Point 1. The cost increment is 27.37% to switch to Point 5, that is actually a high variation. Point 2 has a higher CO₂ emissions than Point 1 because the vessel sails faster outside SECA; also the average sailing speed is slight higher (Figure 6.12). Point 2 remains anyway a cheaper solution for the environment because not only there is a savings in SO₂ emissions, but also because the SO₂ cost has a higher impact than the CO₂ cost. These costs are respectively 12700 [*USD/tonSO₂*] and 37 [*USD/tonCO₂*] (MOVE, 2014). Of course, the environmental benefit depends on how much money the company is willing to pay more. If the national and intentional organizations allocate money as incentive to decrease pollutants emitted, the shipping company will be able to pay more. It is also true that emissions coming from the transportation of goods across the borders cannot be attributed to a specific country, therefore national laws can bring a limited help to the environmental cause.

Environmental safeguard is an international issue; indeed, there are several organizations and committees working on the seaborne trade regulation. Based on the guidelines of the Paris Agreement of 2015, the International Monetary Fund (IMF) suggested implementing a carbon tax of 30 dollars per tonne of CO₂ emitted. This fee can sound quite risible looking at the CO₂ emissions of the shown solutions, but it may be not looking at the whole yearly network of a shipping company. IMF states that \$25 Billion of USD could have been raised in 2014 from the shipping industry business. This tax accord still depends on the collaborative will of the single countries therefore, issuing such duty is far from easy. However, the sulphur Emission Control Areas regulations are currently into force and the shown results consider them. A further analysis has been done on the basis of the new more strict regulations entering into force in 2020. The result is shown in Section 6.7.

Table 6.16: CO₂ and SO₂ emissions of the Pareto Frontier solutions

Point of graph in Figure 6.14	kg of CO₂	tonnes of SO₂
Point 1	14,967.50	2.236
Point 2	15,167.92	2.072
Point 3	11,122.72	1.190
Point 4	11,181.70	1.176
Point 5	8,670.44	0.859
Point 6	6,212.60	0.653
Point 7	6,994.20	0.641
Point 8	5,293.50	0.621

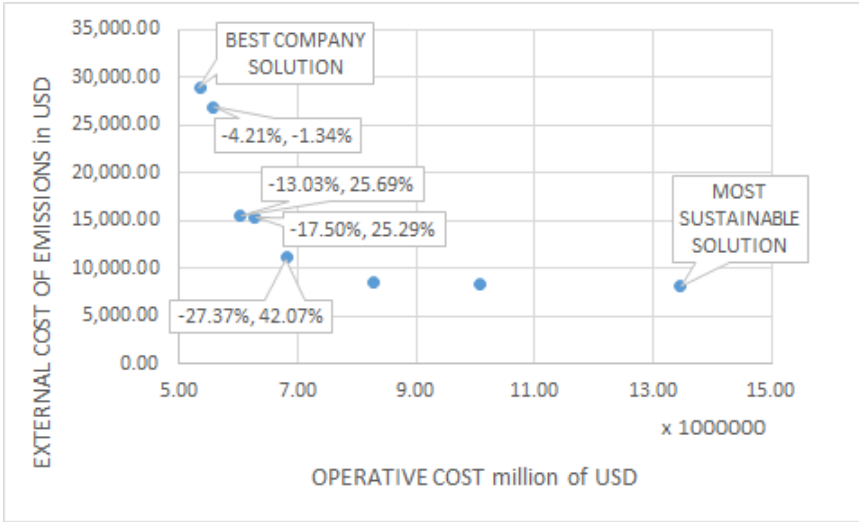


Figure 6.13: CO2 savings in kg of the efficient solutions compared with the company most convenient solution

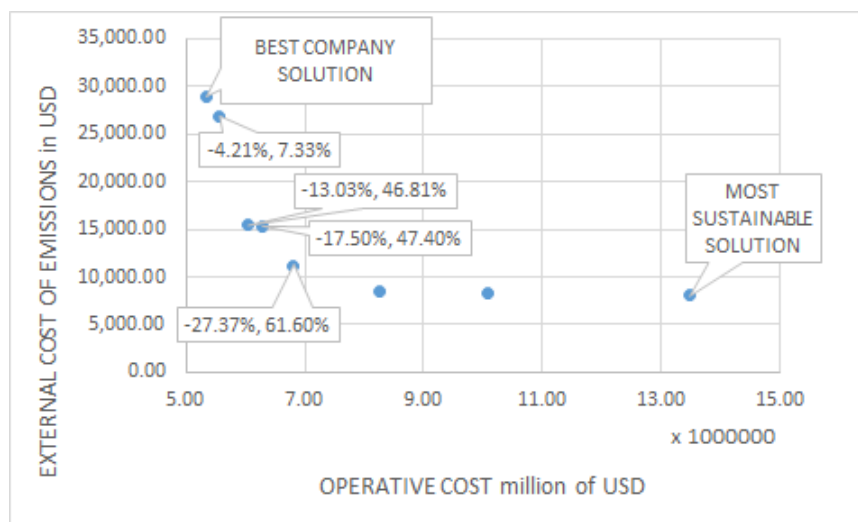


Figure 6.14: SO₂ savings in ton of the efficient solutions compared with the company most convenient solution

6.6 Sensitive Analysis for Delay Cost per Hour per FFE

The cost for the delays has a strong influence on the total cost of the company. For this reason, a sensitive analysis has been done to calculate the operative cost variation for different values of this cost. As stated before, it is difficult to estimate this value; probably the shipping company can do it by looking at its revenue variation when the schedule is not completely respected. The results shown in this report consider a cost of each hour of delay equal to 100 USD per hour per FFE. The cost of delay is calculated in the objective function that minimizes the operative cost for each pair of ports that have a maximum transit time constraint. Of course, it is possible that there is no delay between two ports.

In the other two scenarios proposed, the penalty cost is calculated by accounting 75 and 50 USD per hour of delay. Tables 6.17 and 6.18 compare these two new scenarios with the one used in all the other analysis of this report for the [10Ame] and the [10Atl] instances respectively. As expected, penalty costs results are considerably different, especially for the Atlantic route that has longer distances. The best route that minimizes the operative cost does not change and the low delay fees allow savings in the total costs of the vessel. However, this savings change according to the size of the solved instance. Indeed, while the penalty cost has the same order of magnitude of the bunker cost for the [10Ame], it is the biggest part of the total operative cost for the [10Atl] instance. This is due to the hours of delay that are more in the second instance since distances are bigger.

Another interesting results is that the vessel can slow steam and save bunker cost if the cost of penalty cost decreases. This is true in general but it happens only decreasing the cost from 100 USD to 75 USD in the [10Ame] instance. The reason why the bunker cost do not keep decreasing

in the other cases is that the vessel cost is considered in the operative cost too. If the vessel has to slow steam, there could be the need of sailing for a week more, that means paying an extra 167,000 USD for leasing. Moreover, the length of the route is constrained to be multiple of a week, thus if the vessel has the opportunity to slow steam, it is likely that the penalty cost savings are not enough to let it sail slowly for the whole extra week. Indeed, in the [10Ame] instance, if the cost of delay is 40 [$USD/hour \cdot FFE$], the bunker cost is going to be 1,262,205.26 USD and the route is going to last 7 weeks. The total operative cost keeps decreasing with a value of 3,727,896.53 USD because the savings of bunker and penalty costs are higher than the vessel leasing cost.

In conclusion, the penalty cost is without doubt a key determinant factor for the Liner Shipping Routing and Speed Optimization Problem. A further analysis should be done in order to estimate the cost of delay as better as possible. Also, shipping companies should analyse this cost and try to find the amount that allows the vessel to sail slower in order to save bunker cost.

Table 6.17: Sensitive analysis for the cost of delays, instance: 10 American ports

	100 \$ per hour of delay	75 \$ per hour of delay	50 \$ per hour of delay
Operative cost [USD]	5,344,065.36	4,680,124.00	4,015,794.56
Cost of emissions [USD]	28,953.54	29,022.29	29,022.29
Bunker cost [USD]	1,806,648.16	1,805,135.67	1,805,135.67
Penalty cost [USD]	2,655,417.20	1,992,988.33	1,328,658.89
Vessel cost [USD]	882,000.00	882,000.00	882,000.00
BC [ton]	4,809.19	4,809.19	4,809.19
CO2 emitted [kgCO2]	14,967.50	14,967.54	14,967.54
SO2 emitted [tonSO2]	2.2362	2.2416	2.2416
CO2 emissin cost [USD]	553.80	553.80	553.80
SO2 emission cost [USD]	28,399.75	28,468.49	28,468.49
Weeks	6	6	6

Table 6.18: Sensitive analysis for the cost of delays, instance: 10 Atlantic ports

	100 \$ per hour of delay	75 \$ per hour of delay	50 \$ per hour of delay
Operative cost [USD]	133,088,014.26	101,054,230.17	69,020,446.07
Cost of emissions [USD]	49,539.49	49,539.49	49,539.49
Bunker cost [USD]	3,629,877.89	3,629,877.89	3,629,877.89
Penalty cost [USD]	128,135,136.36	96,101,352.27	64,067,568.18
Vessel cost [USD]	1,323,000.00	1,323,000.00	1,323,000.00
BC [ton]	9,182.96	9,182.96	9,182.96
CO2 emitted [kgCO2]	28,960.60	28,960.60	28,960.60
SO2 emitted [tonSO2]	3.82	3.82	3.82
CO2 emissin cost [USD]	1,071.54	1,071.54	1,071.54
SO2 emission cost [USD]	48,467.94	48,467.94	48,467.94
Weeks	9	9	9

6.7 As-is/To-be Analysis

Figure 1.6 of Chapter 1 depicts the new regulations issued by the IMO, the European Commission and the Hong Kong and China Government Environmental Protection Departments. The limit of sulphur content in the fuel all over the world will be 0.5%, and 0.1% in the Emission Control Areas (ECAs). An As-Is and To-Be analysis has been done in order to evaluate the impact of these

regulations both on the environmental and the company points of view. Table 6.19 shows how some parameters of the model have been modified. The International Bunker Industry Association (IBIA) has provided the potential fuels' costs in 2020, given the new regulations (Association, 2017). Therefore the costs of the fuels inside and outside ECAs have been modified looking at the cited analysis. As regard the CO₂ coefficient to calculate CO₂ emissions, a value of 3.15 has been estimated for the outside Emission Control Areas.

Table 6.19: Parameters comparison between As-Is and To-Be scenarios

	As-Is	To-Be
fuel price inside SECA [USD/ton]	500.00	620.00
fuel price outside SECA [USD/ton]	320.00	570.00
SO ₂ % fuel inside SECA	0.01%	0.01%
SO ₂ % fuel outside SECA	3.50%	0.50%
CO ₂ coefficient fuel inside SECA	3.209	3.209
CO ₂ coefficient fuel outside SECA	3.114	3.150

Tables 6.21 and 6.20 compare the current optimal solution and the optimal solution in 2020 for both the [10Atl] and [10Ame] instances. As expected, the SO₂ emissions in the 2020 will be definitely less than the current optimal solution with the result of a high increment of bunker costs. It is not possible to compare the CO₂ and SO₂ emission costs because the parameters CO_2^{cost} and SO_2^{cost} of Table 4.4 will be different in 2020. Running times of the To-Be scenarios are higher because the complexity of the problem increases since the fuel costs are higher than the As-Is scenario.

Since shipping companies are going to use more expensive fuels, they have to optimize their rotations if they want to save costs and to be competitive in the market. Slow steaming remains without doubts an efficient strategy to deal with the increment of fuel price and it does not require investments. This strategy is of course cheaper than other strategies like designing lighter materials for vessels or installing scrubbers to keep burning non-refined fuel.

Table 6.20: As-Is and To-Be analysis for 10 Atlantic ports instance, obj: operative cost

	As-Is scenario	To-Be scenario	Savings(Loss) Percentage
Route	[1 7 4 2 10 8 5 6 9 3 1]	[1 7 4 2 10 8 5 6 9 3 1]	\
Operative cost [USD]	133,088,014.26	134,884,458.66	-1.35%
Bunker cost [USD]	3,629,877.89	5,426,322.29	-49.49%
Penalty cost [USD]	128,135,136.36	128,135,136.36	0.00%
Vessel cost [USD]	1,323,000.00	1,323,000.00	0.00%
BC [ton]	9,182.96	9,182.96	0.00%
CO ₂ emitted [kgCO ₂]	28,960.60	29,152.92	-0.66%
SO ₂ emitted [tonSO ₂]	3.82	0.61	83.99%
Weeks	9.00	9.00	\

Table 6.21: As-Is and To-Be analysis for 10 American ports instance, obj: operative cost

	As-Is scenario	To-Be scenario	Savings(Loss) Percentage
Route	[1 5 9 10 8 6 7 4 3 2]	[1 5 9 10 8 6 7 4 3 2 1]	\
Operative cost [USD]	5,344,065.36	6,349,360.47	-18.81%
Bunker cost [USD]	1,806,648.16	2,822,787.74	-56.24%
Penalty cost [USD]	2,655,417.20	2,644,572.73	0.41%
Vessel cost [USD]	882,000.00	882,000.00	0.00%
BC [ton]	4,809.19	4,797.06	0.25%
CO2 emitted [kgCO2]	14,967.50	15,215.12	-1.65%
SO2 emitted [tonSO2]	2.24	0.34	84.88%
Weeks	6.00	6.00	\

Chapter 7

Conclusion

The ambition of this thesis was to define a mathematical model to solve the Liner Shipping Routing and Speed Optimization Problem while considering the Emission Control Areas (ECA). ECA are zones where a more refined fuel has to be used in order to limit sulphur emissions. The main issue of the model is to cope with Subtours Elimination Constraints (SEC) and Maximum Transit Time Constraints. Indeed these constraints can be an enormous number according to the size of the instance and the mathematical formulation. The final ambition was to solve instances as large as possible and to analyse the impact of different scenarios on bunker cost and the environment. CO₂ and SO₂ are the pollutants considered in the analysis.

This study was focused on Liner Shipping since it represents a big portion of the international seaborne trade. Moreover, a container ship sails usually at high speeds because its revenue strictly depends on the respect of its schedule. *Slow steaming* is a cheap strategy that allows shipping company to reduce bunker cost and it can be put immediately into practice. The most convenient solution for the shipping company is sailing as slow as possible, that means reducing fuel consumption, with respect to its time schedule. At the same time, vessels' high speed cause high quantity of pollutants; their emission are a significant quantity compared to other shipments. Slow steaming has a strong positive result on the environmental impact as well.

Finding the optimal solution of the LRSOP depends on the size of the instance. Indeed the MTZ's formulation for SEC has been chosen to reduce the number of these constraints, while the number of constraints to find the transit time between ports increase exponentially with the number of ports. Several attempts have been done to decrease the running time of the model and solve instance with more than 10 ports. User Cuts are very effective to tighten the gap between the incumbent solution and the lower bound; in particular, four user cuts strategy have been adopted. The first introduces the DFJ's formulation for SEC that has been proven being stronger than the MTZ's one. This user cut is introduced when a subtour is detected in the LP relaxation. The second and the third user cuts have the purpose of setting lower bounds for the hours of delay and transit time variables. Finally the fourth user cut is introduced when the max flow algorithm identifies a subtour. Unfortunately, even if the user cuts let the solver find higher lower bounds, no one of them improved the running time on the tested instances. Therefore, optimal solutions have been found for instance with 10 ports.

A Bi-Objective Function Model has been used in order to consider both the operative cost and the environmental impact. The latter is measured with the external cost of emissions. The two objective functions propose two substantial different solutions; the Pareto Frontier describes optimal solutions between the most convenient solution for the company and the most sustainable one. As regards the environmental point of view, the results show a clear difference of pollutants emitted between the efficient solutions. Moreover, by making a comparison between the company most convenient solution and another non-dominated point close to the first, savings of CO₂ and SO₂ are

of the order of 25% and 46% respectively with a cost increment of 13% for the company. Further SO₂ savings are shown in the As-Is/To-Be analysis that considers the new sulphur regulations that are going to come into force on 2020. This future SO₂ saving is due to the fact that vessels have to use a more refined and expensive fuel not only in the ECA, but all over the world. CO₂ emissions are not regulated by an international policy, therefore there is not a big difference between the two scenarios of the As-Is/To-Be analysis. Indeed, the different types of fuels produce almost the same CO₂ emissions.

The efficient points of the Pareto Frontier have different average sailing speeds; the lower is the speed, the less is the bunker cost. At the same time, the hours of delay increase if the vessel slows steam. Since the cost per hour per FFE has been estimated, a Sensitive Analysis was done to show the variation of the penalty cost for different values of the parameter. This cost should be estimated as precise as possible in order to evaluate whether the bunker cost savings can cover the expenses for the non-respected maximum transit times.

Two different Heuristic Algorithms have been modelled in order to propose a feasible and good solution for big instances that would require too long running time to be solved until optimality. The model of instances of 20 ports runs for 3 days and the gap is not less than 90%. The described heuristic algorithms are the 2-Steps Method and the Simulated Annealing and they have to be considered as a starting point to be improved in order to find a good solution in reasonable time. Indeed, it is very difficult to find the optimal tuning configuration of the parameters. Both of the algorithms uses an Hill-Climbing algorithm that generates a slight different route in a different way than the classic 2-Opt exchange. In the 2-Steps Method results, three different constructions of the Hill-Climbing algorithm are tested and the best one is found. In the Simulated Annealing there are usually several parameters to tune; in this study only one was tuned, trying to set the others to a reasonable value. However, more instances should be tested to find better configuration of the proposed algorithms; also other metaheuristic techniques that find the local optima and then move on new neighbourhoods may bring better results.

In terms of practical usage of the model, we have to remember that it is based on some hypothesis; for example, the sailing speed is considered constant. These hypothesis are sometimes unavoidable to model the reality. The model reflects the real world and can find optimal solutions of small instances, that are medium-sized routes of 8 or 12 ports. Slow steaming is proven being an effective strategy that the management of shipping companies can use in order to save money and to be competitive on the market. Indeed, it is especially useful when new regulations may limit their profit. Also, the model can be used by policy makers as well; indeed, they can simulate different scenarios according to their regulations and it is possible to analyse the effects on both the environment and the company.

Bibliography

- Aarts, Emile and Jan Korst (1988). “Simulated annealing and Boltzmann machines”. In:
- Acciaro, Michele (2014). “Real option analysis for environmental compliance: LNG and emission control areas”. In: *Transportation Research Part D: Transport and Environment* 28, pp. 41–50.
- Agarwal, Richa and Özlem Ergun (2008). “Mechanism design for a multicommodity flow game in service network alliances”. In: *Operations Research Letters* 36.5, pp. 520–524.
- Alderton, Patrick M (2004). *Reeds sea transport: Operation and economics*. A&C Black.
- Alderton, PM (1981). “The optimum speed of ships”. In: *Journal of Navigation* 34.03, pp. 341–355.
- Álvarez, José Fernando (2009). “Joint routing and deployment of a fleet of container vessels”. In: *Maritime Economics & Logistics* 11.2, pp. 186–208.
- Association, The International Bunker Industry (2017). *How much will 2020 cost?* Available on line. URL: <http://ibia.net/how-much-will-2020-cost/>.
- Aydin, Nursen, H Lee, and SA Mansouri (2017). “Speed optimization and bunkering in liner shipping in the presence of uncertain service times and time windows at ports”. In: *European Journal of Operational Research* 259.1, pp. 143–154.
- Baker, Edward K (1983). “Technical note—an exact algorithm for the time-constrained traveling salesman problem”. In: *Operations Research* 31.5, pp. 938–945.
- Barrass, Bryan (2004). *Ship design and performance for masters and mates*. Butterworth-Heinemann.
- Bertsimas, Dimitris, John Tsitsiklis, et al. (1993). “Simulated annealing”. In: *Statistical science* 8.1, pp. 10–15.
- Brouer, Berit D et al. (2013). “A base integer programming model and benchmark suite for liner-shipping network design”. In: *Transportation Science* 48.2, pp. 281–312.
- BunkerWorld (2017). *Bunkerworld Prices*. Available on line. URL: <http://www.bunkerworld.com/prices>.
- Christiansen, Marielle, Kjetil Fagerholt, Bjørn Nygreen, et al. (2007). “Maritime transportation”. In: *Handbooks in operations research and management science* 14, pp. 189–284.
- (2013). “Ship routing and scheduling in the new millennium”. In: *European Journal of Operational Research* 228.3, pp. 467–483.
- Christiansen, Marielle, Kjetil Fagerholt, and David Ronen (2004). “Ship routing and scheduling: Status and perspectives”. In: *Transportation science* 38.1, pp. 1–18.
- Corbett, James J et al. (2007). “Mortality from ship emissions: a global assessment”. In: *Environmental Science and Technology-Columbus* 41.24, p. 8512.
- Cullinane, Kevin and Sharon Cullinane (2013). “Atmospheric emissions from shipping: The need for regulation and approaches to compliance”. In: *Transport Reviews* 33.4, pp. 377–401.

BIBLIOGRAPHY

- Dithmer, Philip (2015). “Routing and Scheduling of a Liner Shipping Service under Emission Control Policies”. MA thesis.
- DNV (2012). *Shipping 2020*.
- Du, Yuquan et al. (2011). “Berth allocation considering fuel consumption and vessel emissions”. In: *Transportation Research Part E: Logistics and Transportation Review* 47.6, pp. 1021–1037.
- Dunning, Iain (2013). *Using JuMP to Solve a TSP with Lazy Constraints*. Available on line. URL: <http://iaindunning.com/blog/mip-callback.html>.
- Ehrgott, Matthias (2006). “A discussion of scalarization techniques for multiple objective integer programming”. In: *Annals of Operations Research* 147.1, pp. 343–360.
- Ehrgott, Matthias, Xavier Gandibleux, and Anthony Przybylski (2016). “Exact methods for multi-objective combinatorial optimisation”. In: *Multiple Criteria Decision Analysis*. Springer, pp. 817–850.
- Eusébio, Augusto, José Rui Figueira, and Matthias Ehrgott (2014). “On finding representative non-dominated points for bi-objective integer network flow problems”. In: *Computers & Operations Research* 48, pp. 1–10.
- Fagerholt, Kjetil (2001). “Ship scheduling with soft time windows: An optimisation based approach”. In: *European Journal of Operational Research* 131.3, pp. 559–571.
- (2004). “Designing optimal routes in a liner shipping problem”. In: *Maritime Policy & Management* 31.4, pp. 259–268.
- Fagerholt, Kjetil, Nora T Gausel, et al. (2015a). “Maritime routing and speed optimization with emission control areas”. In: *Transportation Research Part C: Emerging Technologies* 52, pp. 57–73.
- (2015b). “Maritime routing and speed optimization with emission control areas”. In: *Transportation Research Part C: Emerging Technologies* 52, pp. 57–73.
- Fagerholt, Kjetil, Gilbert Laporte, and Inge Norstad (2010). “Reducing fuel emissions by optimizing speed on shipping routes”. In: *Journal of the Operational Research Society* 61.3, pp. 523–529.
- Held, Michael and Richard M Karp (1962). “A dynamic programming approach to sequencing problems”. In: *Journal of the Society for Industrial and Applied Mathematics* 10.1, pp. 196–210.
- Hvattum, Lars Magnus et al. (2013). “Analysis of an exact algorithm for the vessel speed optimization problem”. In: *Networks* 62.2, pp. 132–135.
- IMO (2009). *Second IMO Greenhouse Gas Study Study 2009*. Tech. rep.
- (2011). *Low carbon shipping and air pollution control*. URL: <http://www.imo.org/en/MediaCentre/hottopics/ghg/Pages/default.aspx>.
- (2013). *International Maritime Organization, what it is*. URL: http://www.imo.org/en/About/Documents/What%5C%20it%5C%20is%5C%20Oct%5C%202013_Web.pdf.
- (2014). *Third IMO Greenhouse Gas Study 2014 Executive Summary and Final Report*. Tech. rep.
- Kjeldsen, Karina H (2011). “Classification of ship routing and scheduling problems in liner shipping”. In: *Infor* 49.2, p. 139.
- Kontovas, Christos A (2014). “The green ship routing and scheduling problem (GSRSP): a conceptual approach”. In: *Transportation Research Part D: Transport and Environment* 31, pp. 61–69.
- Lee, Chung-Yee, Hau L Lee, and Jiheng Zhang (2015). “The impact of slow ocean steaming on delivery reliability and fuel consumption”. In: *Transportation Research Part E: Logistics and Transportation Review* 76, pp. 176–190.

- Li, Chen, Xiangtong Qi, and Dongping Song (2016). “Real-time schedule recovery in liner shipping service with regular uncertainties and disruption events”. In: *Transportation Research Part B: Methodological* 93, pp. 762–788.
- Lindstad, Haakon, Bjørn E Asbjørnslett, and Anders H Strømman (2011). “Reductions in greenhouse gas emissions and cost by shipping at lower speeds”. In: *Energy Policy* 39.6, pp. 3456–3464.
- MaerskLine (2017). *Maersk Line Annual Report 2016*.
- MaerskLine (2010). *Slow Steaming Here to Stay*. URL: <http://www.maersk.com/en/the-maersk-group/press-room/press-release-archive/2010/9/slow-steaming-here-to-stay>.
- McGranahan, Gordon and Frank Murray (2012). *Air pollution and health in rapidly developing countries*. Earthscan.
- Meng, Qiang et al. (2013). “Containership routing and scheduling in liner shipping: overview and future research directions”. In: *Transportation Science* 48.2, pp. 265–280.
- MOVE, DG (2014). “Update of the handbook on External Costs of Transport”. In: *DG MOVE*.
- Notteboom, Theo E (2006). “The time factor in liner shipping services”. In: *Maritime Economics & Logistics* 8.1, pp. 19–39.
- Notteboom, Theo E and Bert Vernimmen (2009a). “The effect of high fuel costs on liner service configuration in container shipping”. In: *Journal of Transport Geography* 17.5, pp. 325–337.
- (2009b). “The effect of high fuel costs on liner service configuration in container shipping”. In: *Journal of Transport Geography* 17.5, pp. 325–337.
- Öncan, Temel, İ Kuban Altinel, and Gilbert Laporte (2009). “A comparative analysis of several asymmetric traveling salesman problem formulations”. In: *Computers & Operations Research* 36.3, pp. 637–654.
- Padberg, Manfred and Giovanni Rinaldi (1991). “A branch-and-cut algorithm for the resolution of large-scale symmetric traveling salesman problems”. In: *SIAM review* 33.1, pp. 60–100.
- Papadimitriou, Christos H (1977). “The Euclidean travelling salesman problem is NP-complete”. In: *Theoretical computer science* 4.3, pp. 237–244.
- Papadimitriou, Christos H and Kenneth Steiglitz (1977). “On the complexity of local search for the traveling salesman problem”. In: *SIAM Journal on Computing* 6.1, pp. 76–83.
- Pesenti, Raffaele (1995). “Hierarchical resource planning for shipping companies”. In: *European Journal of Operational Research* 86.1, pp. 91–102.
- Premti, Anila (2016). “LINER SHIPPING: IS THERE A WAY FOR MORE COMPETITION?”. In: *United Nation Conference on Trade and Development*.
- Psaraftis, Harilaos N and Christos A Kontovas (2009). “Ship emissions: logistics and other tradeoffs”. In: *10th Int. Marine Design Conference (IMDC 2009), Trondheim, Norway*, pp. 26–29.
- (2013). “Speed models for energy-efficient maritime transportation: A taxonomy and survey”. In: *Transportation Research Part C: Emerging Technologies* 26, pp. 331–351.
- Rana, Krishan and RG Vickson (1991). “Routing container ships using Lagrangean relaxation and decomposition”. In: *Transportation Science* 25.3, pp. 201–214.
- Reinhardt, Line Blander, Tommy Clausen, and David Pisinger (2013). “Synchronized dial-a-ride transportation of disabled passengers at airports”. In: *European Journal of Operational Research* 225.1, pp. 106–117.

BIBLIOGRAPHY

- Reinhardt, Line Blander and David Pisinger (2012). “A branch and cut algorithm for the container shipping network design problem”. In: *Flexible Services and Manufacturing Journal* 24.3, pp. 349–374.
- Reinhardt, Line Blander, Christian EM Plum, et al. (2016). “The liner shipping berth scheduling problem with transit times”. In: *Transportation Research Part E: Logistics and Transportation Review* 86, pp. 116–128.
- Ronen, David (1982a). “The effect of oil price on the optimal speed of ships”. In: *Journal of the Operational Research Society*, pp. 1035–1040.
- (1982b). “The effect of oil price on the optimal speed of ships”. In: *Journal of the Operational Research Society*, pp. 1035–1040.
- (1983). “Cargo ships routing and scheduling: Survey of models and problems”. In: *European Journal of Operational Research* 12.2, pp. 119–126.
- (2011). “The effect of oil price on containership speed and fleet size”. In: *Journal of the Operational Research Society* 62.1, pp. 211–216.
- Sbihi, Abdelkader and Richard W. Eglese (2010). “Combinatorial optimization and Green Logistics”. In: *Annals of Operations Research* 175.1, pp. 159–175. ISSN: 1572-9338. DOI: 10.1007/s10479-009-0651-z. URL: <http://dx.doi.org/10.1007/s10479-009-0651-z>.
- Solomon, Marius M (1987). “Algorithms for the vehicle routing and scheduling problems with time window constraints”. In: *Operations research* 35.2, pp. 254–265.
- Stephan Diederich, University Mannheim (2006). *boykov_kolmogorov_max_flow*. Available on line. URL: http://www.boost.org/doc/libs/1_54_0/libs/graph/doc/boykov_kolmogorov_max_flow.html.
- Stopford, Martin (2009). *Maritime economics 3e*. Routledge.
- UN (2015). “Review of Maritime Transport 2015”. In: *United Nation Conference on Trade and Development*.
- Wang, Shuaian and Qiang Meng (2012a). “Robust schedule design for liner shipping services”. In: *Transportation Research Part E: Logistics and Transportation Review* 48.6, pp. 1093–1106.
- (2012b). “Sailing speed optimization for container ships in a liner shipping network”. In: *Transportation Research Part E: Logistics and Transportation Review* 48.3, pp. 701–714.
- Williams, H Paul (1999). “Model building in mathematical programming”. In:
- WWF (2017). *Living Planet Report 2016*. Tech. rep.
- Zis, Thalys et al. (2016). “Payback Period for Emissions Abatement Alternatives: Role of Regulation and Fuel Prices”. In: *Transportation Research Record: Journal of the Transportation Research Board* 2549, pp. 37–44.